Thermal Analysis, Design and Verification of an Academic CubeSat Mission in a MBSE Context

Thermische Analyse, Entwurf und Verifizierung einer akademischen CubeSat-Mission in einem MBSE-Kontext

Master Thesis by Juan Perales Gómez
Master in Aerospace Engineering
Date of submission: 28/08/2023

1. Supervisor: Marlon Deutsch M.Sc.
2. Supervisor: Prof. Dr.-Ing. Reinhold Bertrand

TECHNISCHE
UNIVERSITÄT
DARMSTADT

FSR

Juan Perales Gómez
Matriculation number: 2833851
Study programme: Master in Aerospace Engineering

Master Thesis
Subject: Thermal Analysis, Design and Verification of an Academic CubeSat Mission in a MBSE Context
Submitted: 28/08/2023
Supervisor: Marlon Deutsch, M.Sc.

Prof. Dr.-Ing. Reinhold Bertrand
Institute of Flight Systems and Automatic Control
Department of Mechanical Engineering
Technische Universität Darmstadt
Otto-Berndt-Str. 2
64287 Darmstadt

Master Thesis

for

Mr. Juan Perales

Matriculation number 2833851

TECHNISCHE
UNIVERSITÄT
DARMSTADT

Subject: **Thermal Analysis, Design, and Verification of an Academic CubeSat Mission in a MBSE Context**

Background

"TUDSaT e.V.", a student association of Technical University of Darmstadt is developing the university's first academic space mission "TRACE" (TU Darmstadt Research CubeSat for Education), a CubeSat which will demonstrate a spin-in technology for ground-based orbit determination as its primary mission. Currently in the preliminary design phase, the satellite is scheduled to launch in late 2024 / early 2025. As a cornerstone of the development approach, the mission team explores and applies model-based systems engineering principles via the platform "Valispace", supported by the institute of flight systems and automatic control (FSR) in an administrative and systems engineering capacity.

Key upcoming steps in the TRACE project include a detailed thermal analysis of the spacecraft in orbit and the planning of related assembly, integration, and verification (AIV) activities. Their formulation, documentation, and integration into the mission's MBSE platform are the main goals of this thesis.
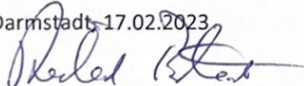
This entails research about the topics of thermal design and verification of space systems as well as model-based systems engineering, the creation of thermal simulations for various orbits and spacecraft configurations, and the detailed formulation of AIV procedures related to the thermal subsystem of TRACE. Where possible, the thesis results and documentation shall be integrated into the mission's Valispace project environment. Additionally, the thesis shall examine the impact of the chosen MBSE approach and its impact on the mission development process. For validation purposes, expert interviews shall be conducted during the course of the thesis.

Tasks

Within this thesis project, the following work packages are defined:

- Literature research about thermal analysis, design, and AIV of space systems, with a focus on small satellites
- Literature research about model-based systems engineering and the MBSE environment chosen for the TRACE mission
- Basic thermal assessment followed by thermal simulations of the spacecraft in representative orbits and hardware configurations
- Detailed definition and formulation of AIV procedures relating to thermal requirements and the thermal subsystem of TRACE
- Integration of developed tools and results into the mission's MBSE environment
- Examination and reflection of the impact of the chosen MBSE approach on the mission development
- Validation via expert interviews
- Documentation and presentation of results

Darmstadt, 17.02.2023

Prof. Dr.-Ing. R. Bertrand

Institut für Flugsysteme und Regelungstechnik

Institute of Flight Systems and Automatic Control

ESA – TU Darmstadt
Joint Professorship
Space Systems

Prof. Dr.-Ing.
Reinhold Bertrand

Otto-Berndt-Str. 2
64287 Darmstadt

Tel. +49 6151 16 - 21047
Fax +49 6151 16 - 21050
bertrand@fsr.tu-darmstadt.de

Marlon Deutsch, M.Sc.
deutsch@fsr.tu-darmstadt.de

Datum
17.02.2023

Thesis Statement

According to § 22 Abs. 7 und § 23 Abs. 7 APB TU Darmstadt

Hiermit versichere ich, Juan Perales Gómez, die vorliegende <Master-Thesis / Bachelor-Thesis> gemäß § 22 Abs. 7 APB der TU Darmstadt ohne Hilfe Dritter und nur mit den angegebenen Quellen und Hilfsmitteln angefertigt zu haben. Alle Stellen, die Quellen entnommen wurden, sind als solche kenntlich gemacht worden. Diese Arbeit hat in gleicher oder ähnlicher Form noch keiner Prüfungsbehörde vorgelegen.

Mir ist bekannt, dass im Falle eines Plagiats (§38 Abs.2 APB) ein Täuschungsversuch vorliegt, der dazu führt, dass die Arbeit mit 5,0 bewertet und damit ein Prüfungsversuch verbraucht wird. Abschlussarbeiten dürfen nur einmal wiederholt werden.

Bei der abgegebenen Thesis stimmen die schriftliche und die zur Archivierung eingereichte elektronische Fassung gemäß § 23 Abs. 7 APB überein.

Bei einer Thesis des Fachbereichs Architektur entspricht die eingereichte elektronische Fassung dem vorgestellten Modell und den vorgelegten Plänen.

Darmstadt, den 28.08.2023

_____
Unterschrift

English translation for information purposes only:

Thesis Statement pursuant to § 22 paragraph 7 and § 23 paragraph 7 of APB TU Darmstadt

I herewith formally declare that I, Juan Perales Gómez, have written the submitted thesis independently pursuant to § 22 paragraph 7 of APB TU Darmstadt. I did not use any outside support except for the quoted literature and other sources mentioned in the paper. I clearly marked and separately listed all of the literature and all of the other sources which I employed when producing this academic work, either literally or in content. This thesis has not been handed in or published before in the same or similar form.

I am aware, that in case of an attempt at deception based on plagiarism (§38 Abs. 2 APB), the thesis would be graded with 5,0 and counted as one failed examination attempt. The thesis may only be repeated once.

In the submitted thesis the written copies and the electronic version for archiving are pursuant to § 23 paragraph 7 of APB identical in content.

For a thesis of the Department of Architecture, the submitted electronic version corresponds to the presented model and the submitted architectural plans.

Abstract

The Thermal Analysis is conducted for the TRACE, the TU Darmstadt Research CubeSat for Education, which is a 2U CubeSat designed by the student association TU Darmstadt Space Technology (TUDSaT) e.V. The project is supported by the German Aerospace Centre (DLR e.V.) and the Institute for Flight Systems and Automatic Control of the Technical University of Darmstadt as well as sponsored by Serco Group Plc.

"Planned to launch in Q4/2024 - Q1/2025, the primary mission of TRACE aims to demonstrate a lightweight and cost-effective technology for passive, laser-based orbit, and attitude determination. The secondary mission is a collaborative project with the Helmholtz Centre for Heavy Ion Research (GSI), that consists of a space weather measurement campaign utilizing a novel sensor technology." [1]

For the thermal analysis, four different cases/modes of the spacecraft are considered: COM (the satellite is only in communication mode), CMEx (the satellite does not communicate, only the cameras and attitude sensors are working), COM_CMEx (the satellite communicates and also uses the cameras and attitude sensors) and finally MAX CHARGE (the satellite faces directly to the Sun light so the batteries inside it can charge). In addition, for each one of these modes, three different attitudes of the spacecraft are taken into account. The first angle of attitude is the desired attitude of the satellite, which is 97,33 degrees. The second one is when the satellite is totally vertical, 90 degrees, and the last one is when the spacecraft is totally horizontal, 0 degrees. For each one of the cases the temperatures are determined for the CubeSat with no thermal control. The obtained temperatures are then compared to the operational typical temperature limits of the most critical on-board components of the spacecraft to try to determine if these components would be able to survive and operate through the course of the specified missions.

Table of Contents

List of Figures

List of Tables

Nomenclature

Symbol Directory

Symbol	Unit	Description
σ	$\dfrac{W}{m^2 \cdot K^4}$	Stefan-Boltzmann Constant
T	K	Temperature
A	m^2	Area
Q	W	Heat Power
q	W/m^2	Heat Flux
α	[-]	Albedo Coefficient
k	$W/m \cdot K$	Thermal Conductivity
R	$Kg \cdot K/J \cdot m$	Resistance
L	m	Longitude
λ	[-]	Absorptivity
ε	[-]	Emissivity

List of Abbreviations

FSR	Institut for Flight Systems and Automatic Control
ESA	European Space Agency
ISS	International Space Station
LEO	Low earth Orbit
COM	Communication Mode of TRACE Satellite
CMEx	TRACE CubeSat only uses cameras and attitude sensors
COM_CMEx	TRACE uses both Communication transceiver and cameras and attitude sensors
MAX_CHARGE	TRACE faces directly to the Sun light to charge its batteries
TUDSaT	TU darmstadt Space Technology
DLR	German Aerospace Centre
TRACE	TU Darmstadt Research CubeSat for Education
ADCS	Attitude Determination and Control Subsystem
PDR	Preliminary Design Review
SLR	Satellite Laser Ranging
GSI	Helmholtz Centre for Heavy Ion Research
MBSE	Model-Based Systems Engineering
RRF	Retroreflective Foil
CCRs	Corner Cube Reflectors

ATCS	Active Thermal Control System
PTCS	Passive Thermal Control System
MLI	Multi-Layer Insulation
PEEK	Polyetheretherketone
AU	Astronomical Unit
Kg	Kilograms
K	Kelvin Degrees
°C	Celsius Degrees
VHF	Very High Frequency
UHF	Ultra High Frequency
iEPS	ISIS Electrical Power System
COTS	Commercial Off-The-Shelf
n.a.	Not Available

1. Introduction

1.1. Motivation and Objective

In the rapidly evolving field of space exploration and satellite technology, CubeSats have emerged as versatile and cost-effective platforms for a wide range of scientific, commercial, and educational missions. These satellites known as CubeSats, that are a class of satellites that adopt a standard size and form factor, which unit is defined as 'U'. A 1U CubeSat is a 10 cm cube with a mass of approximately $2\ kg$ [2], and offers a unique opportunity for researchers and space enthusiasts to conduct experiments and gather valuable data in space environments.
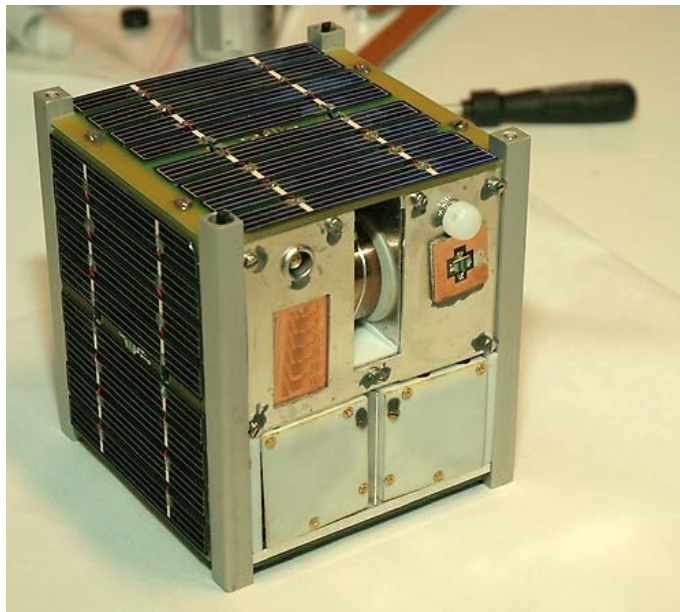
Figure 1: Typical ‚1U' CubeSat.

One of the critical aspects to consider in CubeSat design and operation is thermal management. The temperature variations experienced during different phases of a mission can significantly impact the satellite's performance and reliability. Understanding and predicting the thermal behaviour of CubeSats under various operating conditions is essential to ensure their successful mission execution and prolonged lifespan.

This Master's Thesis aims to conduct a comprehensive thermal analysis of the 2U CubeSat built by the student association TUDSAT within the scope of the TRACE mission, focusing on evaluating its thermal behaviour under diverse operating modes of the satellite. The study investigates the satellite's response to thermal loads during COM, CMEx, COM_CMEx and MAX_CHARGE modes. By performing a detailed analysis, the project intends to identify potential thermal challenges and develop effective thermal control strategies to maintain the CubeSat's temperature within operational limits.

To achieve this objective, various analytical and numerical methods would typically be employed, including Finite Element Analysis (FEA) and Computational Fluid Dynamics (CFD). However, due to unforeseen licensing

issues with the required software packages, the direct implementation of FEA and CFD simulations was regrettably not feasible for this study. Nevertheless, the project leverages alternative approaches to achieve meaningful insights into the CubeSat's thermal behaviour.

The findings from this thermal analysis, albeit without FEA and CFD simulations, contribute to enhancing the design and operational guidelines for future CubeSat missions. The study's outcomes enable researchers and engineers to develop more robust and efficient satellite systems, while also shedding light on the impact of thermal management on the success of CubeSat missions.

The subsequent sections of this report delve into the methodology, data analysis, and results obtained from the experimental thermal analysis of the 2U CubeSat under different conditions. The conclusions drawn from the study provide valuable insights for the space community, paving the way for more sophisticated and successful CubeSat missions in the future.

1.2. Definition of a CubeSat

As previously stated, a CubeSat is a class of satellites that adopt a standard size and form factor, which unit is defined as 'U'. A 1U CubeSat is a 10 cm cube with a mass of up to 2 kg. [3] They often use off-the-shelf components and are launched as secondary payloads on large rockets launching much larger spacecrafts. Around 1,600 CubeSats have been launched to date. [4] Initially designed by professors Jordi Puig-Suari from California Polytechnic State University (Cal Poly) and Bob Twiggs from Stanford University Space Systems Development Laboratory in 1999, CubeSats were meant to foster skills for small satellite design and research. While initially academic, their uses have expanded to scientific experiments, Earth observation, and technology demonstrations. Notably, they've been used for deep space missions and even served as a country's first satellite. Thanks to the low price of the satellite and the launch opportunities offered by major launch providers and manufacturers CubeSats are an ideal method for educational purposes, so with the appearance of CubeSats, the space is now fully opened to everyone. [3]

Referring to the launch opportunity, the majority of CubeSats are carried out to orbit as secondary spacecraft, using the excess launch capability of larger rockets. This method of carrying out CubeSats to orbit is known as "Rideshare Launches". The idea of ridesharing consists of a primary mission with excess of mass, volume, and performance margins which are used by another spacecraft. Secondary spacecrafts are also called auxiliary spacecraft or piggyback spacecraft. In the case of educational CubeSats, several initiatives help provide this launch opportunities. [5] For example, NASA's CubeSat launch initiative (CSLI) provides low-cost access to space for U.S. educational institutions, informal educational institutions such as museums and science centres, non-profits with an education/outreach component, and NASA centres for early career workforce development. CSLI intent is to inspire and develop the next generation of scientists, engineers, and technologists by offering a unique opportunity to conduct scientific research and develop/demonstrate novel technologies in space. [6] As of October 2022, CSLI launched 148 CubeSats, and continues to select CubeSats for launch. [7] In the case of Europe, "Fly Your Satellite" program, from ESA, is a similar program as CSLI, with the objective to complement academic education and inspire, engage, and better prepare university students for a more effective introduction to their future professions in the space sector. [8]

The commonly referred-to basic CubeSat unit is the '1U,' with dimensions of 10x10x10 cm, which can be scaled in increments of 0.5U, 1U or more, facilitating the creation of larger versions, such as a '1.5U' version. Notably, there are instances of '2U' CubeSats (20x10x10 cm) and '3U' CubeSats (30x10x10 cm), which have been developed and effectively launched, but CubeSats can be as large as a '12U' CubeSat, as it can be seen in Figure 2. [3]
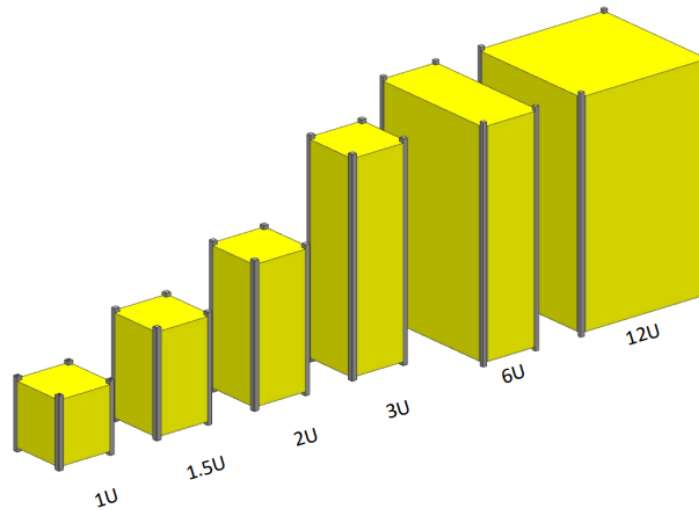
Figure 2: Current CubeSat Family (1U-12U) [3]

Since almost all the CubeSats are standardized with 10 cm x 10 cm (regardless of length), they would also need a standard flight-proven CubeSat deployment system. This would lead to a better integrity, so the people involved in the project would only have to deal with one type of system. The standardization would benefit both the manufacturers and the launcher companies. The most common standard system is the P-POD (Poly Pico-Satellite Orbital Deployer) from Cal Poly. Each Payload Pod (P-POD) is crafted to accommodate three standard CubeSats and serves as the crucial link connecting these CubeSats with the launch vehicle. Constructed as a rectangular aluminium tubular frame, it integrates an electronically activated door mechanism equipped with spring-loading. Upon activation, the door releases the CubeSats, which are then propelled by the spring along designated guidance rails. This mechanism achieves the deployment of the CubeSats into orbit at a separation speed of a few meters per second. [9] The P-POD is designed to accommodate up to three 1U CubeSats. Nevertheless, due to the size equivalencies, it offers flexibility in deploying CubeSats. This adaptability stems from the fact that the deployment combination can range from 1U to 3U, as three 1U CubeSats occupy the same space as a single 3U CubeSat, and two 1U CubeSats match the size of a 2U CubeSat. [10]
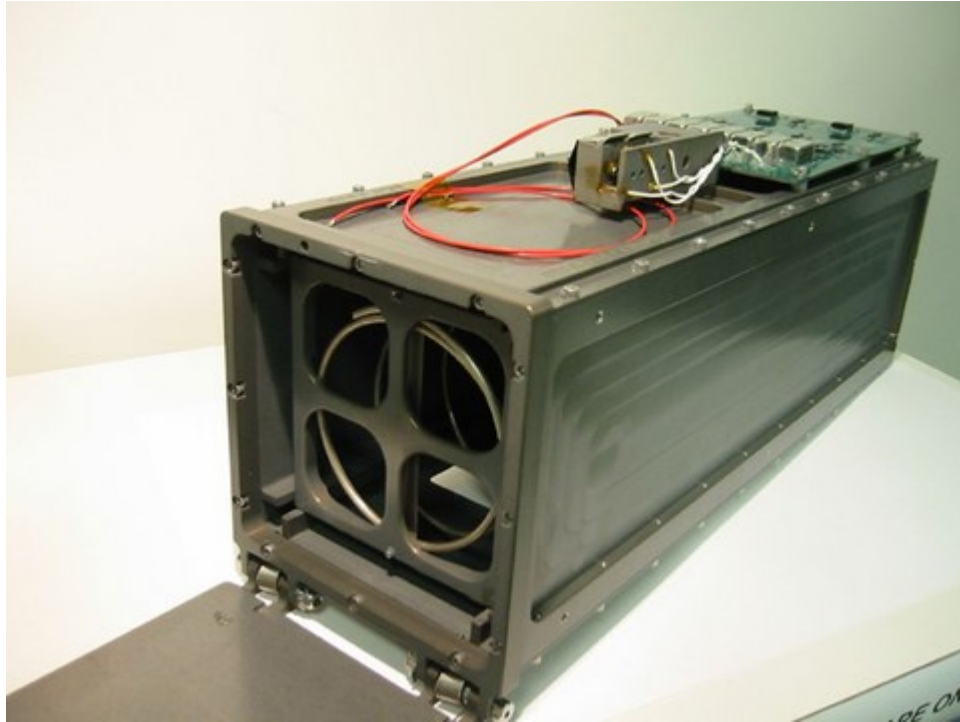
Figure 3: Standard P-POD. [11]

As stated before, the principle of standardization often aligns with adaptability. Utilizing pre-qualified P-POD and launch vehicle interfaces optimizes mission compatibility, reducing integration timelines and financial outlays. This approach also streamlines design, analysis, and testing for future missions, leveraging repetitive frameworks. Furthermore, it provides added advantages such as the option to relocate CubeSats to an alternative launch vehicle if there are launch postponements or cancellations. [12]

Educational payload components require their own power sources and communication capabilities. There are no electrical connections to the CubeSats from either the P-POD or the main payload. Once a CubeSat is inserted into the P-POD prior to launch, subsequent battery charging is not possible. The CubeSats are expected to remain electrically passive within the P-POD, exhibiting no power dissipation or radiofrequency emissions. Their operation is projected to commence using the sensors in the CubeSat structure's feet to gauge launcher separation. [12]

Despite a notable rise in launch costs across various providers, CubeSats remain the most economical way to independently launch payloads into orbit. Many companies and research institutions offer clustered launch opportunities, applying the cost distribution concept to reduce final outlays. This approach involves distributing costs among multiple customers, deploying multiple spacecraft through a single mechanism, and employing standardized systems instead of bespoke equipment. [5] [13] [14] [15]

In summary, CubeSats are a series of miniaturized standardized satellites used for scientific purposes or experiments, technology demonstrations, and Earth observation. Their standardized design and cost-effective launches make them accessible for various purposes.

1.3. History of CubeSats

The initiation of CubeSats commenced in 1999 when professors Jordi Puig-Suari of California Polytechnic State University (Cal Poly) and Bob Twiggs of Stanford University developed CubeSat specifications in order to promote and develop the skills necessary for creating small satellites intended for LEO operations. They proposed a reference design for the CubeSat, with its main objective in mind to enable graduate students to design, build, test and operate limited capabilities of artificial satellites within the time and financial constraints of a graduate degree program. [3]

The first launched CubeSats were placed into orbit in June 2003 from Russia's Plesetsk launch site. At the time, the going rate for a CubeSat's launch was about $40,000 [16], which is a bargain compared to a typical satellite, which can be millions of dollars. Starting on 2013, the number of launches suddenly numbered in the dozen, due to the fact that in that year the commercial sector began to launch satellites. [17] Since that date, and until mid-2018, more than 2100 CubeSats and nanosatellites have been placed into orbit for educational and research purposes. [4]

CubeSat applications usually involve experiments which can be miniaturized and provide services for earth observation and amateur radio applications. Some CubeSats are used to demonstrate spacecraft technologies or as feasibility demonstrators that can help to justify the cost of a larger satellite. [2]

In some cases, CubeSats may be used for low-cost scientific experiments that may verify underlying theories. In many cases, CubeSats represent a first national satellite for non-spacefaring nations. Finally, several future missions to the Moon and beyond are in the planning stages for CubeSats.

CubeSats have allowed the creation of an entire spaceflight subculture. Since it only takes one or two years to build and launch these tiny spacecrafts, and the cost is only a small fraction of money spent on traditional satellites, many more people have entered the space exploitation community. For example, university students can see the results of their work while still working on degrees. Of course, these advantages have also led to important innovations. [6]

The applications of CubeSats range from technology experiments to biological research. In this field it should be remarked the AeroCube mission as a technology experiment and demonstration of CubeSats and the GeneSat mission as an astrobiology experiment. A short list of CubeSats applications and some examples of CubeSat missions with the corresponding application is shown below. [18]

- Technology Experiment and Demonstration
  - AeroCube
- Scientific Research
  - SWISSCube – 1
  - ION
  - CanX – 2
  - QuakSat
- Biological Experiments

- o GeneSat
- o PharmaSat
- o O/OREOS
- Earth Remote Sensing
  - o CSSWE CubeSat

Some present and future missions from ESA involving CubeSats include [19]:

- RACE: ESA's Rendezvous Autonomous CubeSats Experiment will test out autonomous rendezvous and docking capabilities for CubeSats.
- QARMAN: launched from the International Space Station (ISS) in spring 2020, QARMAN is demonstrating re-entry technologies, particularly novel heatshield materials, a new passive aerodynamic drag stabilisation system, and the transmission of telemetry data during re-entry via data relay satellites in LEO.
- PRETTY: PRETTY will demonstrate a novel technique used primarily to detect sea ice and test a miniaturised radiation dosimeter. It is due to launch later in 2022.

1.4. TU Darmstadt Research CubeSat for Education (TRACE)

TRACE, the TU Darmstadt research CubeSat for Education, is a 2U CubeSat designed by the student association TU Darmstadt Space Technology (TUDSaT) and supported by the German Aerospace Centre (DLR) and the Institute for Flight Systems and Automatic Control of TU Darmstadt as well as sponsored by Serco Group Plc. [1]

TRACE has two main missions. The primary mission is to demonstrate technology of retroreflective foils, which are commonly applied in other industries (e.g., for street signs), for laser-based orbit and attitude determination using SLR stations. Its secondary mission is to perform a campaign of space weather measurement with novel and lightweight sensor technology by GSI. [1]

There have been some key development steps leading up to PDR for the TRACE [1]:

- A re-design from 1U to 2U CubeSat form factor, that started in February 2023, due to thermal, power, configuration, and interference concerns (see Figure 4 and Figure 5 for the initial and final design of TRACE CubeSat respectively, and Figure 6 for the final dimensions of TRACE CubeSat).
- The dedicated "TRACE Lab" at the Lichtwiese campus in TU Darmstadt is currently under renovation, and it will be available approximately in April 2023, so it cannot be used until then.
- There has been a migration to a model-based systems engineering (MBSE) environment using Valispace to apply and exploit the MBSE functionalities that it provides.

Figure 4: Initial design of TRACE CubeSat. [1]
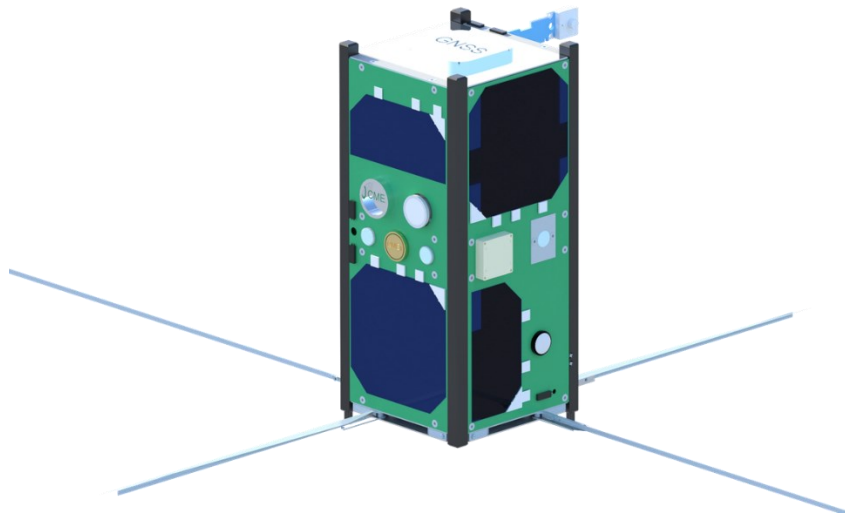
Figure 5: Final design of TRACE CubeSat. [1]
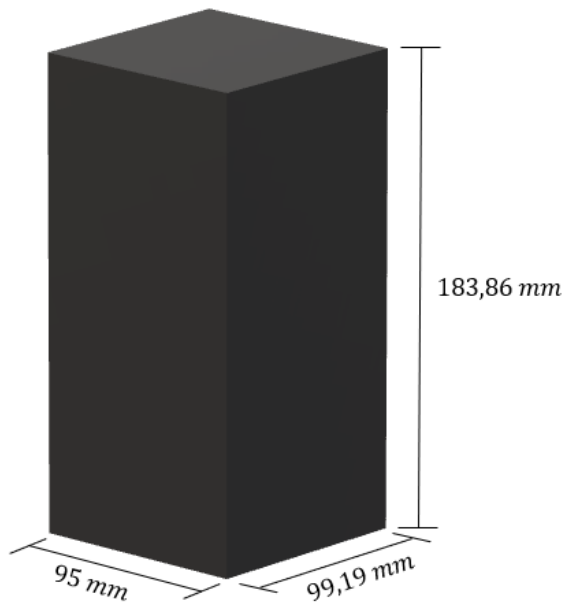
Figure 6: Diagram with the dimensions of TRACE CubeSat.

The TRACE CubeSat consists of the following subsystems:

- ADC: Attitude Determination and Control (it also includes orbit determination)
- COM: Communication
- OBDH: On-Board Data Handling
- PAY: Payload
- PWR: Power
- STM: Structures and Mechanisms
- THE: Thermal Control

The internal components of the TRACE CubeSat can be seen in Figure 7.
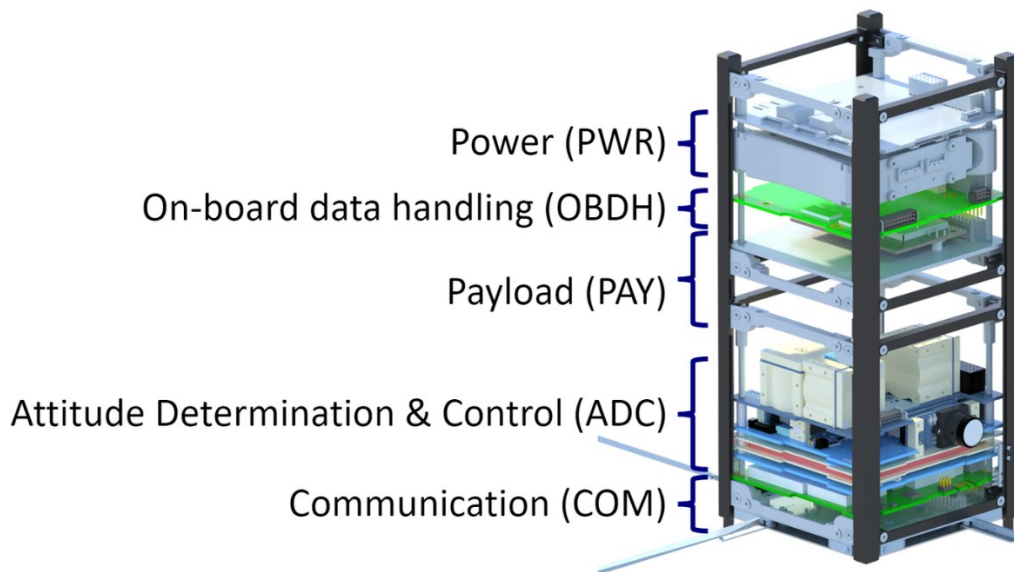
Figure 7: Main components of TRACE CubeSat. [1]

TRACE's main missions are explained in more detail below.

1.4.1. Primary Mission

As stated before, the primary mission objective is the demonstration of retroreflective foil (RRF) for passive, laser-based tracking of objects in low earth orbits.

Presently, there exist numerous satellites incorporating corner cube reflectors (CCRs) in orbital operations, representing the current standard for passive optical identification. For instance, TECHNOSAT by TU Berlin utilizes CCRs for this purpose. Nevertheless, CCRs possess larger dimensions and greater mass that the proposed retroreflective foil (RRF) solution. Additionally, CCRs necessitate housing and attachment to the CubeSat framework. In contrast, the RRF can be affixed to external surfaces and compatible components, potentially offering a more convenient and accessible means to precisely track both active space systems, like satellites, and appropriately equipped passive objects in orbit. In order to assess RRF's performance against a reliable reference dataset, CCRs are also integrated into the TRACE system for comparison. [1]

If the RRF performs as anticipated, this cost-effective and lightweight technology holds the potential for future application in accurately tracking non-cooperative entities, such as defunct satellites or space debris.

During the primary mission, two key objectives will be demonstrated:

- Initially, it will be shown that the foil generates a signal of sufficient strength to undergo processing by the ground based SLR stations. Algorithms designed for orbit determination based on CCR returns will be utilized with this signal to showcase their mutual compatibility. [1]
- Furthermore, distinct patterns exhibited by both RRF and CCRs on the CubeSat will facilitate the analysis of satellite attitude and rotation solely through the SLR signal. This data will subsequently be compared to in-situ ADC information. This insight could be employed for diagnostic purposes in cases where communication with the satellite is unfeasible, or for strategic planning concerning active space debris elimination or the prediction of space debris orbit and deorbit scenarios. [1]

Figure 8: Retroreflective foil (RRF) patterns on TRACE CubeSat. [1]

Figure 9: Corner Cube Reflectors (CCRs) on TRACE CubeSat. [1]

1.4.2. Secondary Mission

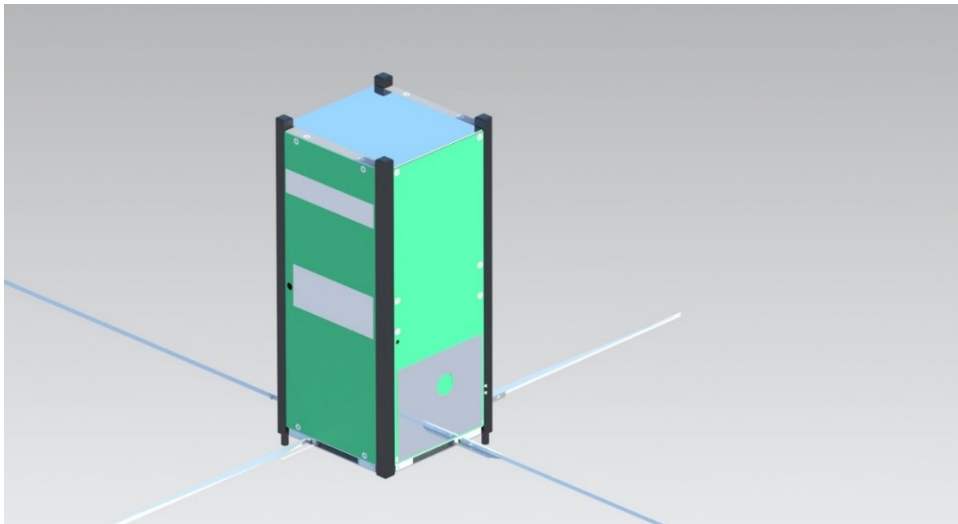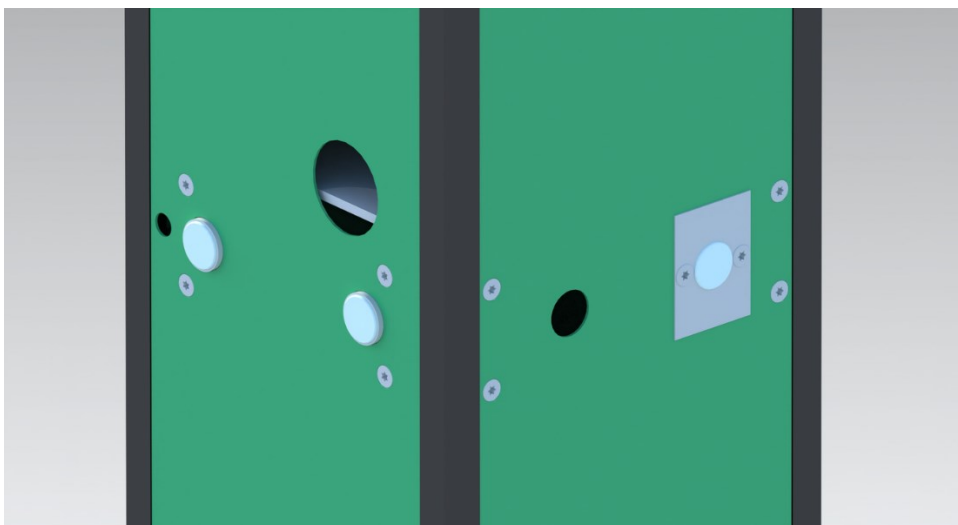As a secondary mission of TRACE, two spacecraft sensors are dedicated to the analysis of "space weather". Collaborating to achieve this objective are a commercially available gamma radiation monitoring module (GRM) and a charge amplifier (CMEx), developed by GSI in Darmstadt for their FAIR particle accelerator. [1]

By translating the collected data from both modules into a global space weather map, it becomes possible to scrutinize potential irregularities and temporal variations. Furthermore, this mapped GRM data could enhance the precision of predicting the radiation tolerance required for electronic components intended for deployment in low earth orbit (LEO). Given the compact nature of CMEx and its relative simplicity compared to prevailing components, the CubeSat's small size and cost-effectiveness make it an ideal platform for such endeavours. This module's successful deployment might even pave the way for future satellite use, facilitating diverse data collection for multiple orbits. [1]

Space weather remains a domain rich with unexplored facets, aided by missions like Parker Solar Probe and Solar Orbiter that continually furnish fresh solar data. In closer proximity to Earth, LEO satellites can amass congruent data for correlation with solar activity measurements. This correlation could prove increasingly valuable considering the anticipated surge in solar activity over the coming years. [1]
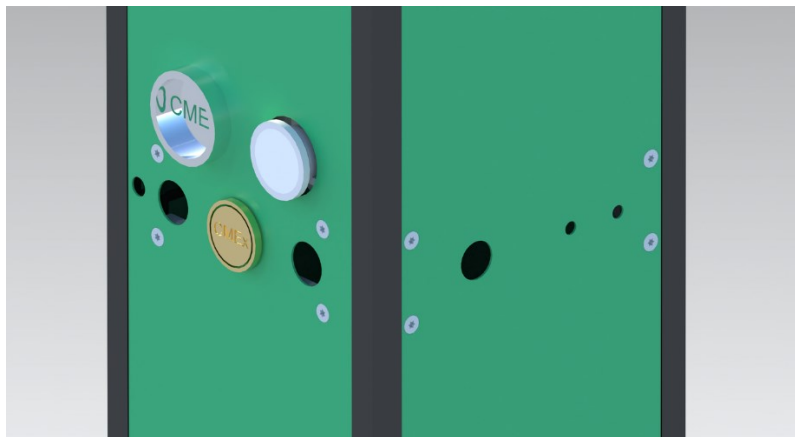
Figure 10: External sensors and cameras payloads of TRACE CubeSat. [1]

1.5. Methods for Thermal Control

As stated previously, one of the main subsystems of the TRACE CubeSat is the Thermal Control Subsystem. Some measures for thermal control of CubeSats are discussed below.

The Thermal Control Subsystem (TCS) of a satellite can be passive, active or a combination of both. When the thermal control is done by using moving fluids or mechanisms, or power, it is called Active Thermal Control System. This is achieved through conductive and radiative heat path. It involves mechanically pumped fluid or heating elements to perform heat transfer. ATCS can handle large heat loads and provides a degree of control over how to manage heat loads. Generally, ATCS is not developed in case of nanosatellites, such as CubeSats, due to its high-power requirement and a high increase in mass and mechanical complexities. [20]
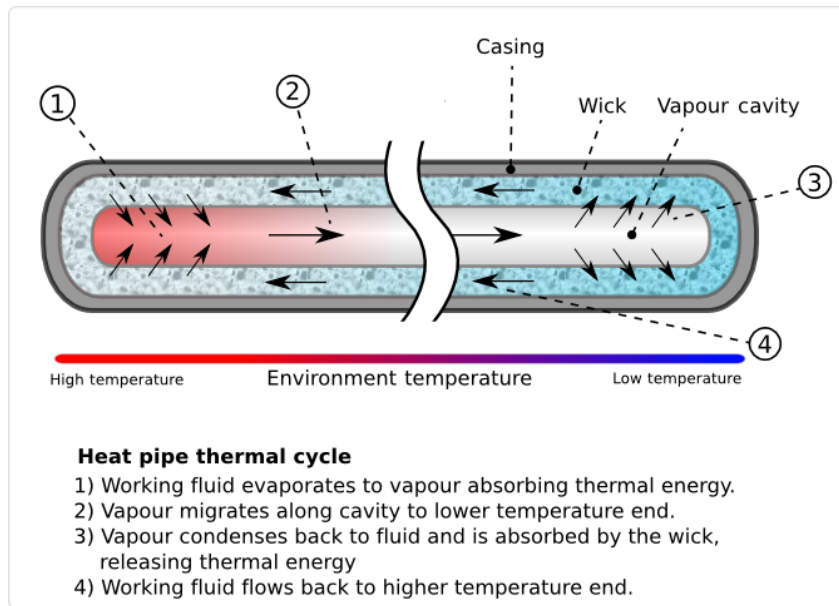
Figure 11: Heat pipe cycle and mechanism. [20]

As it has been previously stated, active thermal control system is not used in CubeSats due to its high complexity and increase in mass, only passive thermal control system is used for this type of satellites. Passive thermal control systems involve no mechanical moving parts or fluids, and there is no power consumption which ensures its low mass and cost. It is highly reliable due to its design simplicity, implementation, and testing. The only drawback of PTCS is its low heat transport capability when compared to ATCS. Due to this advantages, passive thermal control systems are the perfect choice for thermal control of CubeSats. [21]

The passive thermal control subsystem may consist of the following components:
- Thermal Insulations
- Surface Coatings and Paints
- Phase Change Materials

Thermal insulation utilizes low-conductivity materials combined to attain lower overall thermal conductivity. Various insulation forms, such as fibre, powder, and flake types, incorporate solid materials within air spaces. This results in an effective thermal conductivity, dependent on material attributes, void characteristics, and volume ratio. Bulk density, intricately linked to material packing, holds particular importance. "Cellular insulations" pertain to systems where sealed voids form rigid matrices, exemplified by plastic and glass-based foamed systems. Reflective insulations encompass parallel, layered foils that reflect energy, with foil spacing hindering air movement and sometimes evacuated in high-performance insulation. This air within void spaces reduces overall thermal conductivity, considering modes like conduction, convection, and radiation. These intricate processes collectively shape the effective thermal conductivity assessment. [21]

The most common thermal insulation used in satellites is the Multi-Layer Insulation (MLI) (Figure 13). Multi-Layer Insulation (MLI) is a key strategy for temperature management and heat transfer control within satellites. MLI blankets offer dual protection by preventing excessive heat loss from satellite components and mitigating excessive heating due to external environmental fluxes and other sources. The integration of radiators for waste heat dissipation often requires cutouts in the MLI. For scenarios where reduced thermal insulation suffices, lightweight and cost-effective single-layer radiation barriers can be employed as alternatives to MLI.

Nevertheless, simply increasing the number of MLI layers does not lead to improved performance. As layer count rises, the significance of radiative heat transfer diminishes compared to conductive "shorts" between layers and other losses. Generally, a balance is struck at around 25 layers to achieve the optimal overall conductance (Figure 12). [21]

Figure 12: Multi-Layer Insulation Close-Up. [21]

Multi-Layer Insulation (MLI) is fashioned from numerous layers of low-emittance films, often using vacuum-deposited aluminium on Mylar sheets. This layered structure functions as a thermal insulator, curtailing conductive heat transfer pathways between layers. Mylar serves as a spacer, while enhanced performance can be achieved with double-sided metalized Mylar and low-conductance spacers like silk or Dacron net. Heat transfer in MLI involves solid conduction, radiation, and gaseous conduction, all addressed through strategies like reflective surfaces and sparse spacers. Minimizing contact is key to reducing solid conduction. Since these heat transfer mechanisms coexist and interact, using an apparent thermal conductivity or effective emittance becomes valuable for characterizing MLI's thermal behaviour. [21]

During satellite launches, MLI contains air that needs to escape harmlessly as the rocket ascends through the atmosphere. This necessity introduces holes or perforations in layers, albeit at the cost of reduced effectiveness. Traditional MLI crafting involves layer cutting, stacking, and sewing at edges. However, seams and gaps in insulation are responsible for significant heat leakage. A fresh approach involves using polyetheretherketone (PEEK) tag pins to secure film layers, improving thermal performance compared to sewing. In certain scenarios, insulating layers might require grounding to prevent charge buildup and radio interference. MLI can also serve as an initial defence against dust impacts. [21]
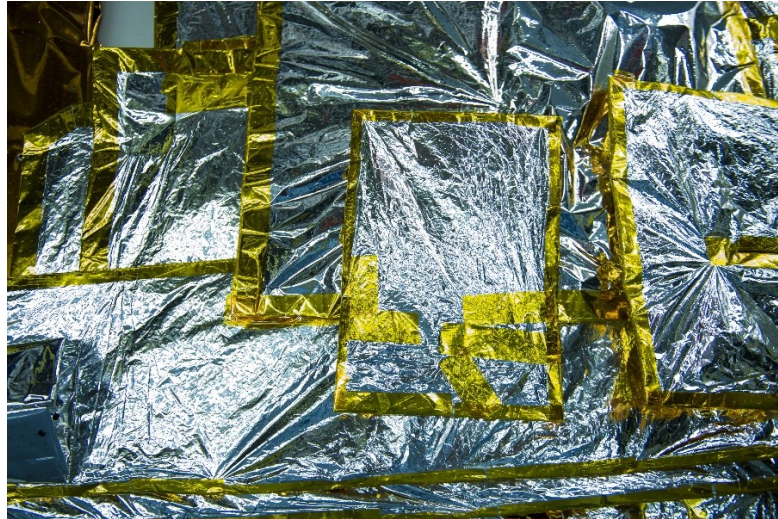
Figure 13: Multi-Layer Insulation Blankets. [22]

Another passive thermal control system component is the surface coatings and paints. The surface finishes of satellites and space stations vary due to the diverse thermal requirements across their configurations. Proper selection of thermal coatings and paints must ensure compatibility with the surrounding environment, as well as resistance to the continuous exposure to radiation and atomic oxygen. Various finishes serve the purpose of providing differing levels of thermal control for onboard equipment. By utilizing coatings and paints with distinct emissivity and absorptivity characteristics, specific regions or components can be thermally adjusted, either increasing or decreasing their temperatures as needed. For example, radiators may incorporate coatings with high emissivity and low absorptivity to effectively dissipate excess heat into space. [21]

The last passive thermal control system component which is discussed in this document is the Phase Change Materials. This novel technology aims to provide effective thermal management by maintaining a constant temperature heat source or sink for a wide range of electronic components in rapidly changing thermal conditions. The proposed Phase Change Material (PCM) panel is designed to be lightweight and flexible, while still possessing substantial thermal capacity. [21] This results in lower mass and volume requirements compared to traditional carbon-fibre and aluminium honeycomb composite panels. [23] For example, Roccor LLC of Longmont, Colo., incorporates phase change material in a device intended to regulate internal heat in low-orbit satellites. This product utilizes a flat structure containing paraffin wax. When the satellite experiences elevated temperatures, the paraffin wax functions as a heat sink, transitioning into a liquid state to store energy. Later, this stored heat is released to maintain stable temperatures within the satellite. [24]
PCM represents an evolving area in the realm of efficient passive thermal control systems, offering the versatility to act as both a heat sink and a heat source based on the system's requirements.
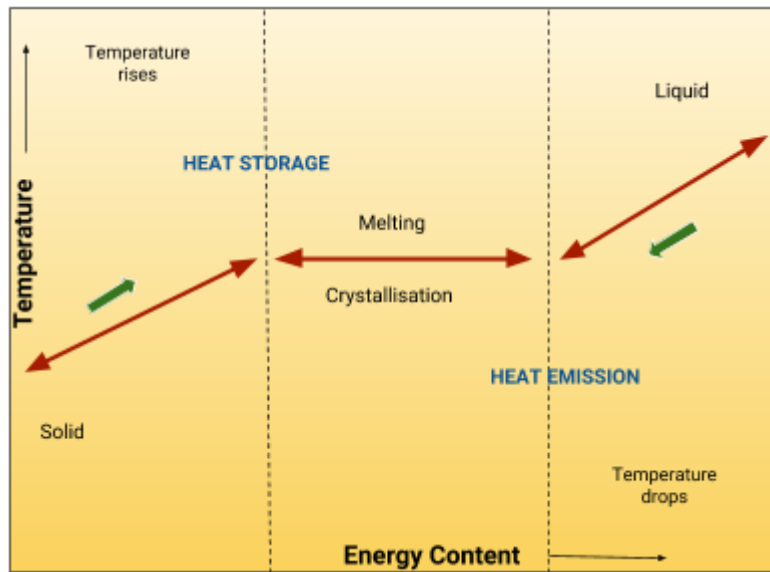
Figure 14: Principle of Phase Change Materials. [21]

Figure 15: Paraffin Wax. [25]

2. Space Environment

There exist three ways of heat transfer: conduction, convection, and radiation.

Conduction is the process by which heat is transferred from the hotter end to the colder end of an object. The ability that the object possesses to conduct heat is known as thermal conductivity. Heat spontaneously flows along a temperature gradient. In the case of an absence of an opposing external driving energy source, temperature differences decay over time, and finally thermal equilibrium is achieved, the temperature becoming much more uniform. In conduction, the heat flow occurs within and through the body itself. If the body is a solid, conduction is generated by the combination of vibrations and collisions of the molecules. In the case of gases or liquids, conduction happens due to the collision and diffusion of the molecules during their random motion. [26]

Convection is the transfer of heat due to the motion of a fluid, such as liquids or gases. This means that heat transfer due to convection cannot occur in solid bodies. As a region of the fluid heats up, its molecules gain energy and become less dense, causing the fluid to expand and rise. Conversely, cooler regions of the fluid are denser and tend to sink. This results in a continuous circulation of the fluid, known as convection currents, which facilitate the transfer of heat from the warmer areas to the cooler ones. In the realm of heat transfer, convection plays a pivotal role in various natural and engineered systems, including atmospheric processes, ocean currents and heat exchangers. [27]

Radiation refers to the process by which energy in the form of electromagnetic waves is emitted from a surface due to the temperature of that surface. As previously mentioned, conduction and convection need a medium for heat transfer, but in the case of radiation, it can occur through a vacuum, as it relies on the emission and absorption of electromagnetic radiation. This phenomenon follows the principles of blackbody radiation, that state that an object with a temperature higher than absolute zero emits thermal radiation. Radiation is characterized by its unique properties, including its dependence on temperature and surface properties. The intensity and spectrum of the emitted radiation are determined by the temperature and emissivity of the emitting surface. The Stefan-Boltzmann Law describes the total power that is radiated by a blackbody depending on its temperature, and the Planck's Law describes the spectral distribution of its radiation. Understanding radiation is critical for various applications, such as the optimization of energy-efficient building or the design of thermal control systems of spacecrafts. [28]

The TUDSaT CubeSat (TRACE) is designed to be in a Low Earth Orbit (LEO) with the variables of the orbit are represented in , and three different attitudes of TRACE in this orbit, 97,33 $degrees$, 90 degrees and 0 degrees, are studied to see the influence of the satellite's attitude as it can be seen in Figure 16. As it can be seen in Figure 16, the attitudes of 90 and 0 degrees have some of the satellite's faces pointed directly to the three main heat sources that exist in space near Earth, the first one being the direct solar radiation. As the Sun being the brightest and closest body in the solar system, it is the greatest source of thermal radiation towards the satellite. At a mean distance of 1 AU, the average heat intensity of solar radiation is approximately 1366.1 W/m^2 (q_{sun}). [29] The second heat source is the Earth's infrared radiation, which consists of the sunlight that is absorbed by

the earth's surface and then it is reemitted towards the space. The last one is the radiation known as albedo, which is the portion of radiation that is reflected by a surface in comparison to the total incident radiation. [27] It is expressed as a value between 0 and 1, and this value depends, in the case of the Earth, on clouds, forests, oceans and polar cap seen. [29] In case of an eclipse, the spacecraft does not receive any radiation from the Sun, and therefore neither from the albedo, it does only receive the Earth's infrared radiation, as a spacecraft is always exposed to this radiation. All these heat sources are clearly visible in Figure 17. Adding to these three sources of radiation that the spacecraft receives, it is also taken into account the heat that is emitted directly from the spacecraft. This heat is due to the fact that most of the components of the satellite consume power, and for the sake of simplification, during this work the heat that is radiated from the spacecraft is the same as the power consumed in each one of the different operating modes of the TUDSaT spacecraft, as stated in the previous section.

Keplerian Element	Value
Altitude	480.00 km
Semi-Major Axis	6858.10 km
Eccentricity	0.00
Inclination	97.33 °
LTAN/RAAN	6 Pm
Argument of Perigee	n. a.

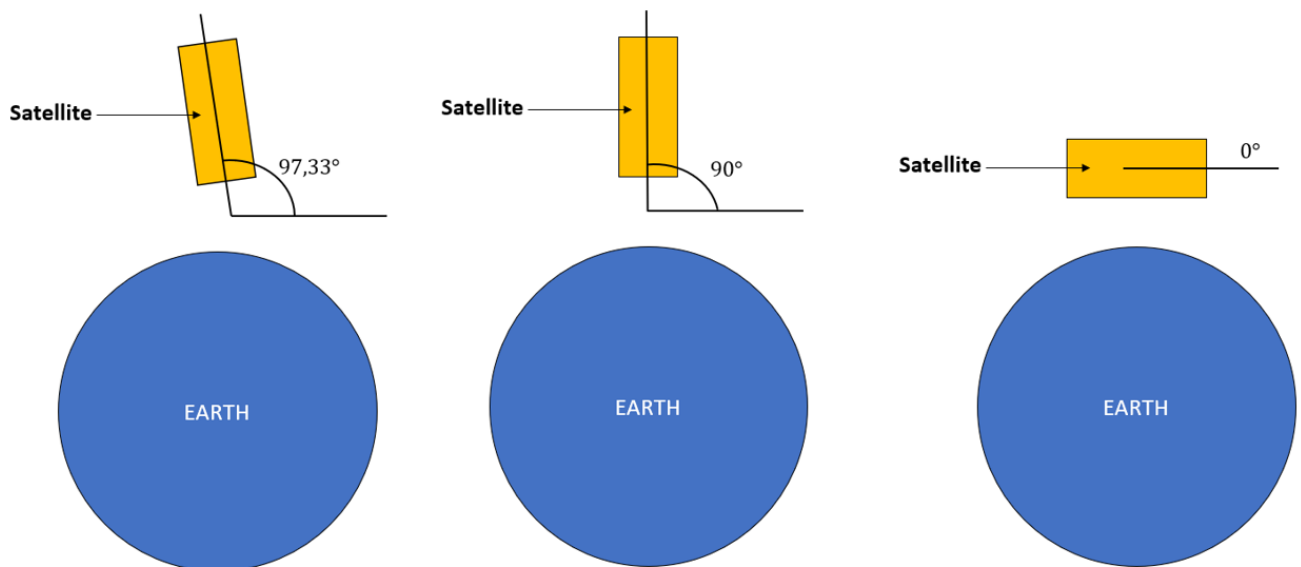Table 1: Values of the Keplerian elements of TRACE's desired orbit. [1]

Figure 16: The three different attitudes that are studied for TRACE satellite.
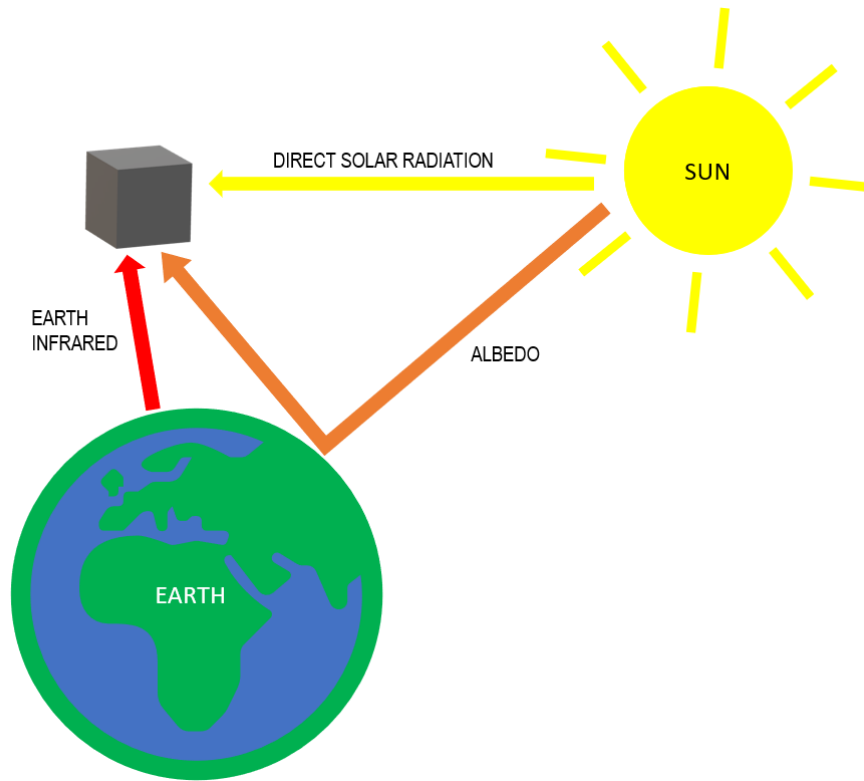
Figure 17: Thermal space environment of the satellite.

In addition to these different operating modes of the spacecraft, two different calculation states are considered: the steady state of the spacecraft, where it is located in one point of the orbit, receiving all the radiation from the heat sources mentioned above, and the second one is a transient state, where TRACE CubeSat is driving along its desired orbit.

2.1. Steady State Thermal Analysis: Theory

As a preliminary step for determining the temperature of the spacecraft surface, a steady state thermal analysis is to be performed. As it has been stated previously, there exist three different types of heat transfer: conduction, convection, and radiation, and more concretely in the case that concerns us, the direct solar heating Q_{sun}, the Earth albedo heating Q_{albedo} and finally the Earth's infrared heating Q_{earth}. The different formulas of these three different types of heat sources are being described in the following. [29]

$$Q_{sun} = A_{sun} \cdot q_{sun} \tag{1}$$

$$Q_{albedo} = A_{albedo} \cdot \alpha \cdot q_{sun} \cdot F_{12} \tag{2}$$

$$Q_{Earth} = A_{Earth} \cdot \sigma \cdot T^4 \cdot F_{12} \tag{3}$$

As it can be seen in these formulas, all the equations depend on three different areas (A_{sun}, A_{albedo}, A_{Earth}). These areas represent the area of the spacecraft that each one of the heat sources 'see', and obviously, they depend on the attitude of the satellite. It can also be seen that in the case of the albedo, it depends on two more

dimensionless factors, known as the albedo coefficient (α) and the 'view factor' coefficient (F_{12}). The albedo is heavily dependent on the landscapes such as clouds or forests, as previously stated. This albedo coefficient can vary from 0.05 to 0.8 depending on the landscape (Figure 18), and in the case that concerns us, a value of 0.6 is taken into account. The view factor represents the amount of radiation that leaves one surface and that arrives directly to another surface. It also takes into account the relative positions, shapes, and orientations of the surfaces, affecting how much radiation emitted by one surface is intercepted by the other surface. [27] The view factor is only used in the calculations of the albedo and the Earth infrared, because solar radiation is often treated differently due to its directional nature and its dominant source (the sun), while albedo and infrared radiation require consideration of the view factor due to their complex interactions between various surfaces within a system.
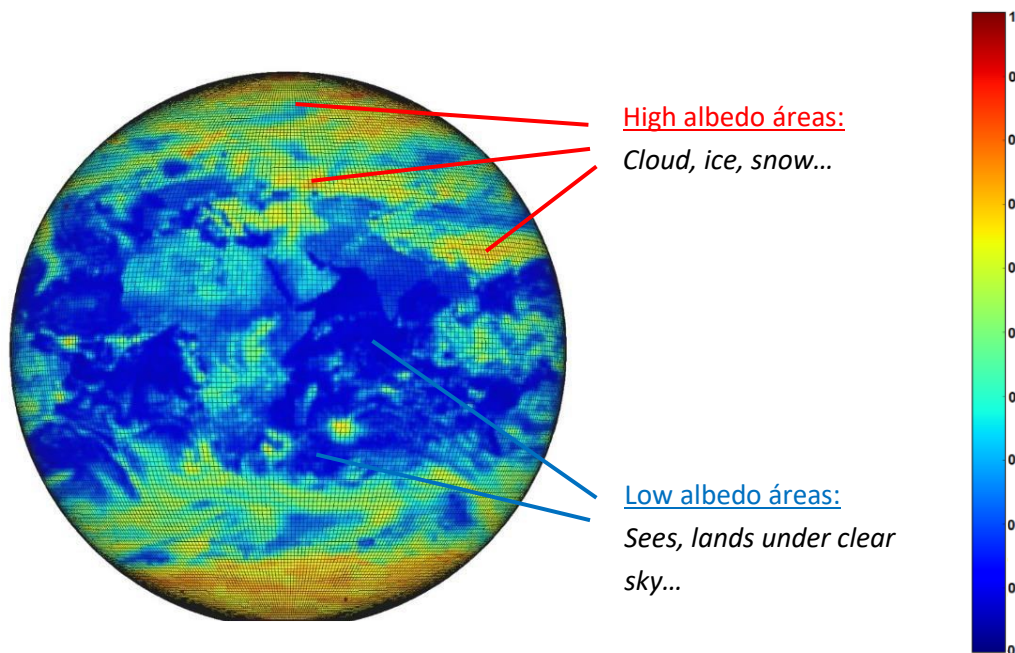

Figure 18: Different zones and values for the albedo radiation. [29]

For the calculation of the view factor, the ECSS regulations is followed. [30] In this case, the equation for the view factor is the one for a planar to spherical surface, because our satellite has planar faces, and the emitting object that needs to be considered is spherical (the Earth). Figure 19 shows the diagram that represents the case of our study.
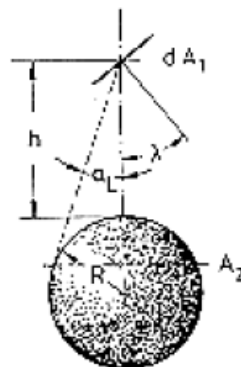

Figure 19: Diagram of the Planar to Spherical case to calculate the view factor. [30]

$$F_{12} = \frac{\cos \lambda}{(1 + H)^2} \tag{4}$$

Where $H = h/R$, h is the height of the orbit and R is the radius of the Earth, which is 6378 km.

Additionally, in the case of the Earth infrared, the equation includes another coefficient, which is the Stefan-Boltzmann constant (σ). This is because the Earth is considered as a black body $(\lambda = \varepsilon = 1)$ that emits radiation, so the equation uses the Stefan-Boltzmann constant and also the temperature of the black body. In this case, two different temperatures are considered: 260 K for the hot case and 240 K for the cold case. [29]

All the radiation coming from these three heat sources need to be added together and are named Q_{ext}. For the calculation of the temperature of the surface of the satellite, the heat that is coming from the inside of the satellite due to the working components needs also to be taken into account, and as has previously been told, the TRACE satellite has 4 different operating modes, and they are named Q_{mode}. This heat, for simplification purposes, is considered exactly the same as the power consumption of the components in each different mode, as stated previously, and also the satellite is considered a black body, as the Earth $(\lambda = \varepsilon = 1)$. This power consumptions of the main components of the satellite are described in Table 2.

		Operating Modes			
		COM	CMEx	COM_CMEx	MAX_CHARGE
	ADCS	1,055	1,055	1,055	1,055
	Transceiver	0,612	0,612	0,612	0,612
Components	PAY	0,0038	0,2438	0,2438	0,0038
	OBC	0,4	0,4	0,4	0,4
	PWR	0,093	0,093	0,093	0,093
	TOTAL	2,1638	2,4038	2,4038	2,1638

Table 2: Values of the power consumption in [W] for each one of the operating modes. [1]

Once the heat that comes from the exterior (Sun, Albedo and Infrared) and the heat that comes from the interior (components in the different modes) are known, they need to be added up and matched with the heat that the satellite is capable of emitting (Q_{out}). This heat that the satellite emits has almost the same equation form as the Earth infrared, but in this case the view factor is not taken into account and the temperature of the deep space needs to be used (T_{inf}). The temperature of deep space is supposed to be 3 K. [29] So finally, the equation takes the following form:

$$Q_{out} = A_{tot} \cdot \sigma \cdot \left(T_s^4 - T_{inf}^4\right) \tag{5}$$

In equation (5), the area that is used is the total area of the satellite. This is because it's all the satellite that is emitting (each one of the faces is considered to emit exactly the same amount of heat, for simplification purposes), not only one or two faces of it. Finally, the variable T_s is the temperature of the surface of the satellite

and is the value that needs to be determined. To do so, the equation to determine the temperature of the surface is the following one:

$$Q_{ext} + Q_{mode} = Q_{out} \tag{6}$$

For this purpose, 4 different operating modes of the satellite are taken into account, as previously mentioned, and for each one of these operating modes two cases are studied: a hot case and a cold case. For the hot case, the hottest temperature of the Earth's surface is used ($260\ K$), and for the coldest case the temperature of the Earth's surface that is used is the coldest one ($240\ K$). During these two cases, all the external heat (Solar, Albedo and Infrared) is considered because as the satellite is in a LEO and Sun synchronous Orbit, the satellite is never in shadow (eclipse).

2.2. Transient State Thermal Analysis: Theory

The surface temperature determined by equation (6) provides a foundation for the thermal analysis of a spacecraft, but it does not provide an exact representation of what it actually occurs thermally to the satellite during orbit. The equation (6) is used for calculating the temperature of the satellite's surface at a specific point while it is assumed that the satellite is stationary at one point of the orbit, but in reality, the temperature of the satellites does not reach the hot or cold temperature instantaneously while going through its own orbit. Therefore, an analysis to study how the temperature of the satellite evolves during its orbit must be performed.

Because this is a hard process to calculate, an application designed by Bruno Mattos for MATLAB is used. [31] This application simplifies the calculation of the transient thermal analysis using the Lumped Parameter Model. Even though this application is quite powerful, it has a limitation, and that is the number of CubeSat configurations. In this application, a 2U CubeSat cannot be calculated, only 1U, 3U, 6U or 12U. With this limitation in mind, a 1U CubeSat is used for this calculation, and this 1U CubeSat has all the same dimensions and material properties as TRACE's CubeSat. Another limitation of the application is the lack of possibility to modify the attitude of the satellite, so in this transient state analysis the albedo is the variable that is studied, to see its influence in the satellite's temperature.

The Lumped Parameter Model is a simplified approach used in thermal analysis to predict the temperature behaviour of a solid object, in this case the 2U TRACE CubeSat, by considering it as a single, uniform entity with homogeneous thermal properties. In this model, the object is divided into discrete volumes or "lumps" that are assumed to have uniform temperature distribution within each lump. Heat transfer within and between these lumps is characterized using thermal capacitance and thermal resistance concepts. [32]

The lumped parameter model assumes that the temperature variation within each lump is negligible over the timescales of interest, allowing the temperature within the lump to be represented by a single value. Heat conduction, convection, and radiation within and between the lumps are modelled using simplified equations based on the lump's thermal properties. [32]

In this case, as the object of analysis is a 2U CubeSat, the model used in the MATLAB application and transient thermal analysis has 7 lumps, as it can be seen in Figure 20.
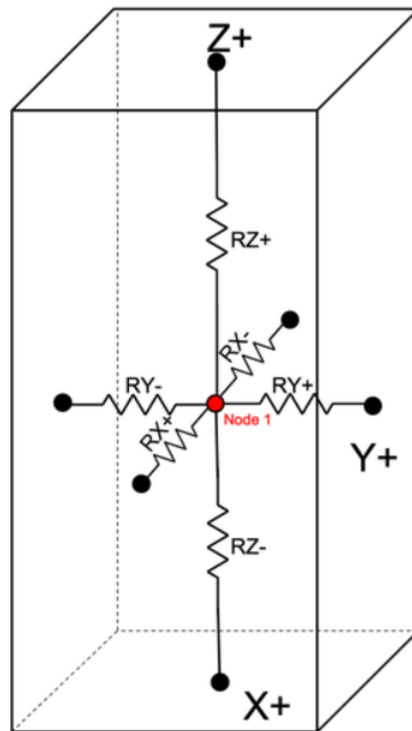

Figure 20: Diagram of the lumped parameter model for a 2U CubeSat.

The thermal resistances needed to link each one of the lumps to the central one are described in the following equation. [32]

$$R = \frac{L_c}{k \cdot A} \tag{7}$$

The equation (7) is the equation to calculate the thermal resistance in conduction, because it is happening inside the satellite due to all its components, and these components transfer their heat with conduction because they are in contact with the surfaces of the satellite and between other components.

The equation (7) includes the variable L_c, that represents the longitude from the central lump to the other lumps, the variable A represents the total area of the face of the lump that its resistance is being calculated, and finally the thermal coefficient 'k' of the material of the face that includes the lump of the resistance that is being calculated.

In the case of the thermal coefficient, also known as thermal conductivity, two different values are considered. For the case of the faces of the TRACE satellite where solar panels exist, the assumption that the entire face is composed of such panels is made, for more simplified calculations. Therefore, the thermal conductivity is that of the solar panels used in the construction of the TRACE satellite. In the faces that do not exist solar panels, the thermal conductivity is obtained with the mean value of the thermal conductivity of the most important and

bigger components found in TRACE CubeSat. The solar panels used for the TRACE satellite are COTS assemblies from Azur Space, which are GaAs cells with an efficiency of 29,3 %. [33]

Below, Figure 21 and Figure 22 show the TRACE satellite with all the faces that possess solar panels. As it can be seen, there is only one face that does not possess any solar panels. In Table 3, the values of mass and thermal conductivity that are used for the transient calculations are shown in Table 3.

		Mass [g]	Thermal Conductivity $\left[\frac{W}{m \cdot K}\right]$
Aluminium	Structure	206	170
	ADCS	561	170
PCBs		300	0,25
Solar Panels		52,8	46
Batteries		310	30
Transceiver		75	0,25

Table 3: Mass and Specific Heat of the main materials of the principal components. [1] [34] [35] [36]

All the thermal conductivities that are used and can be found in Table 3 are considered to be the thermal conductivities of the main material that the component is made of. The ADCS (Attitude Determination and Control Subsystem) main material is the aluminium, as well as the structure for the TRACE CubeSat. [37] In the case of PCBs, their main material is FR-4 [38] [39], with the conductivity shown in Table 3 . For the solar panels, as they are made of GaAs (Gallium Arsenide) [33], their main material is GaAs and thus its thermal conductivity is the one of the GaAs. [35] The batteries are Lithium-Ion Batteries, so the thermal conductivity is shown in Table 3. [40] Finally, the main material in the transceiver used for TRACE CubeSat is the PCBs, so the thermal conductivity that is used for the calculations is the same as the PCBs as is shown in Table 3.
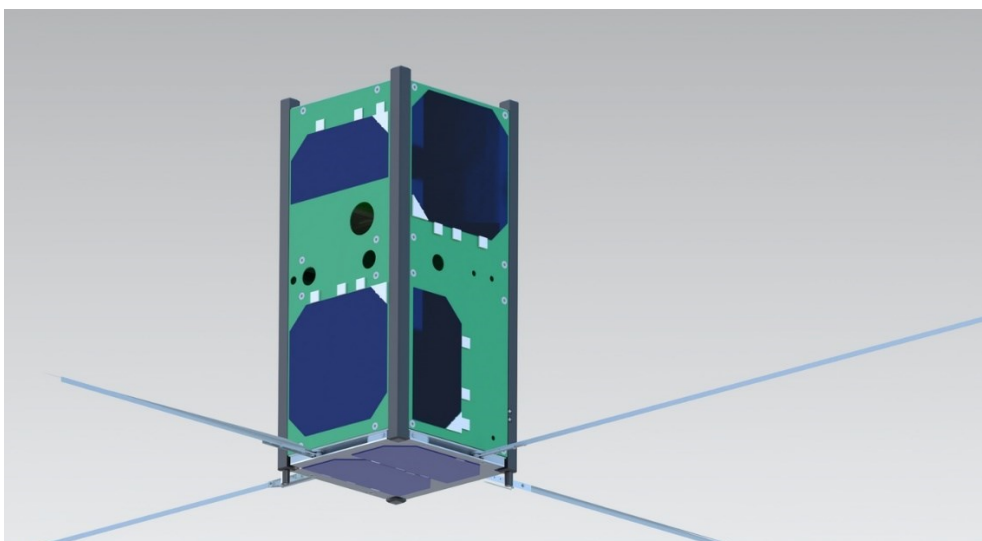

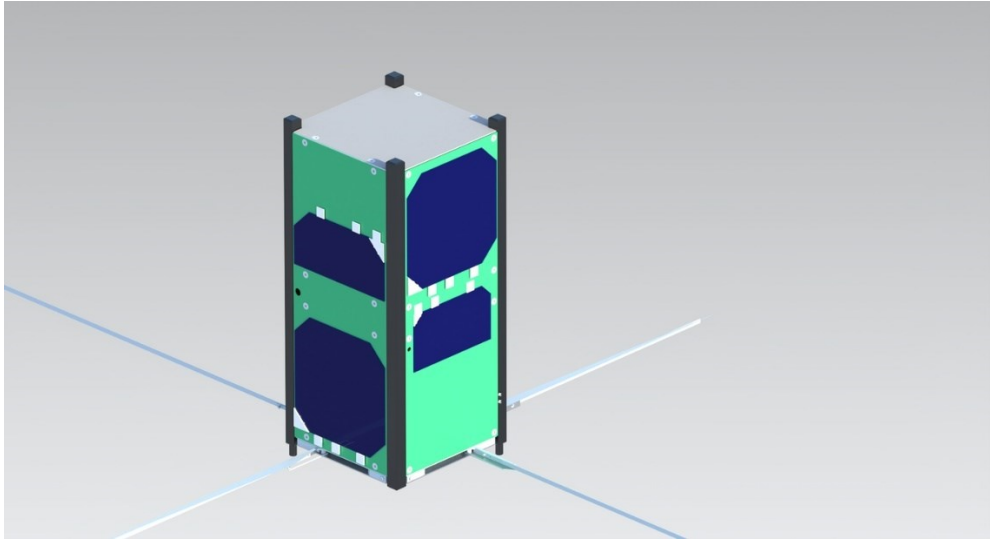Figure 21: Solar cells present on X+, Y+, Z- of TRACE CubeSat. [1]

Figure 22: Solar cells present on X-, Y- of TRACE CubeSat. [1]

3. Results

In this section, all the results are presented and briefly discussed. The results are presented individually for each one of the four operating modes and for the two different cases: hot and cold case. For the hot case, as previously stated, a temperature of the Earth's surface of 260 K is assumed, while for the cold case a temperature of 240 K is assumed.

3.1. Steady Thermal Analysis Results

These results are obtained following the procedure described in the section 2.1, and they are presented independently for each one of the four operating modes. Also, three different attitudes for each one of the operating modes, as previously mentioned, are considered.

3.1.1. COM Mode

For the COM (Communication) mode, the cameras that are included in the payload component are not on, and thus they do not consume any power, as it can be seen in Table 2.

Applying the procedure described in section 2.1, the results for the steady state thermal analysis in the case of COM mode can be seen in the following figures.
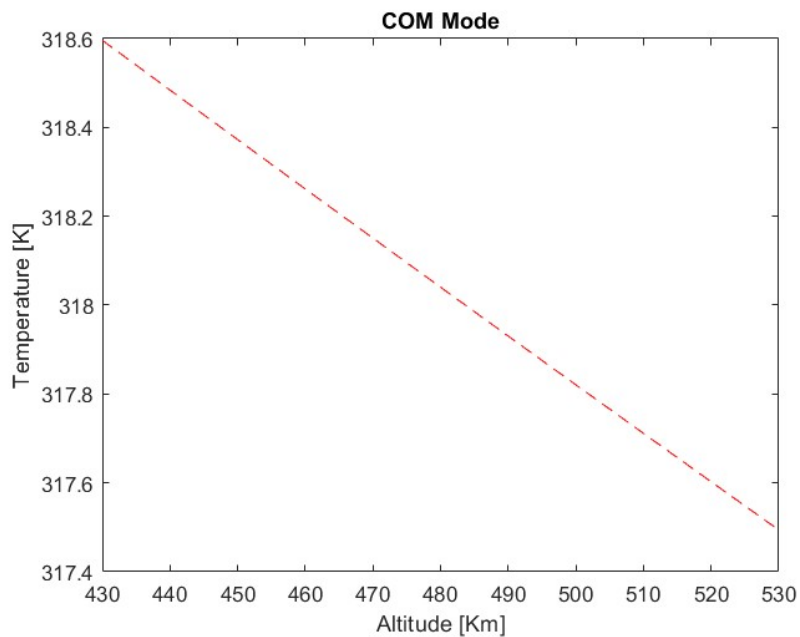
Figure 23: Results obtained for COM Mode in hot case (260 K) and satellite's attitude of 97,33 degrees.
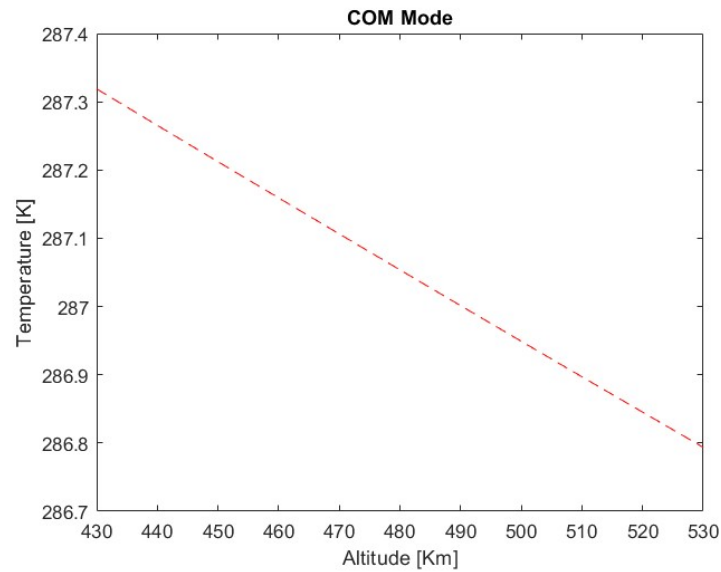
Figure 24: Results obtained for COM Mode in hot case (260 K) and satellite's attitude of 90 degrees.
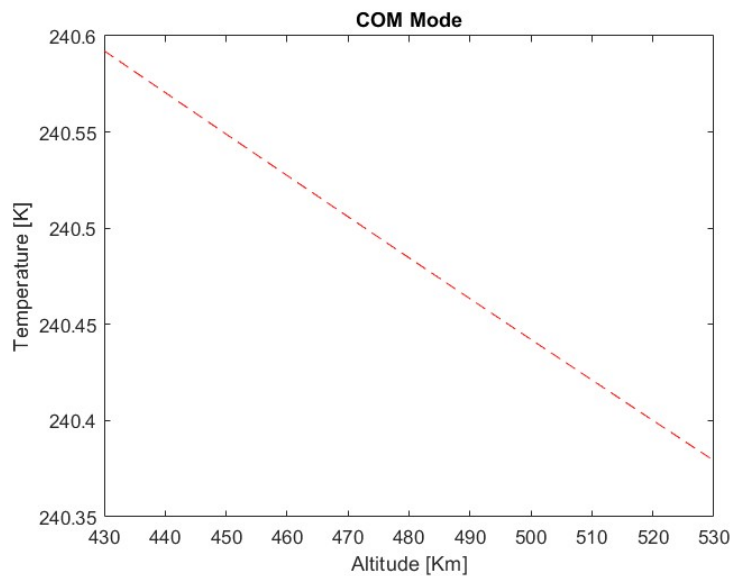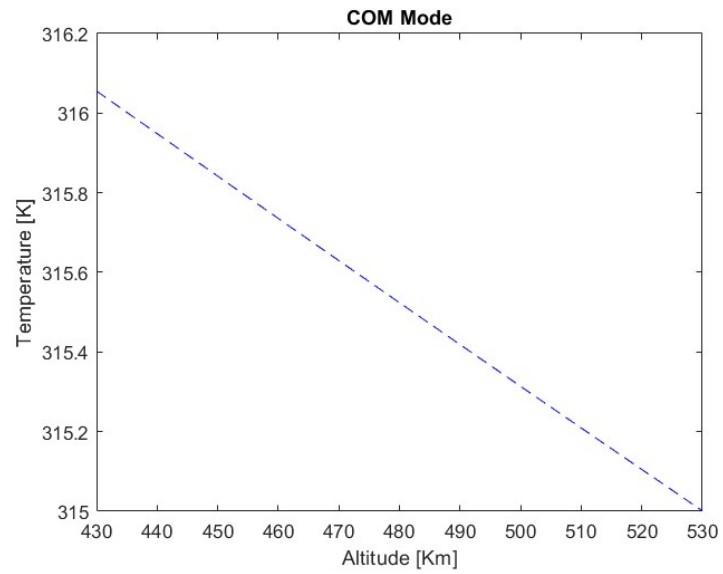

Figure 25: Results obtained for COM Mode in hot case (260 K) and satellite's attitude of 0 degrees.

As it can be seen in Figure 23, Figure 24 and Figure 25, the temperature decreases as the altitude of the satellite increases. This is due to the decrease of the view factor from equation (4) as the altitude increases. Another thing that can be observed is that the satellite's attitude has an enormous impact on its surface temperature. When the satellite is in its desired attitude, its temperature is more than 318 K (45 °C), and as the angle of attitude decreases, the temperature also decreases until a very low point where the temperature is less than 241 K (-32 °C).

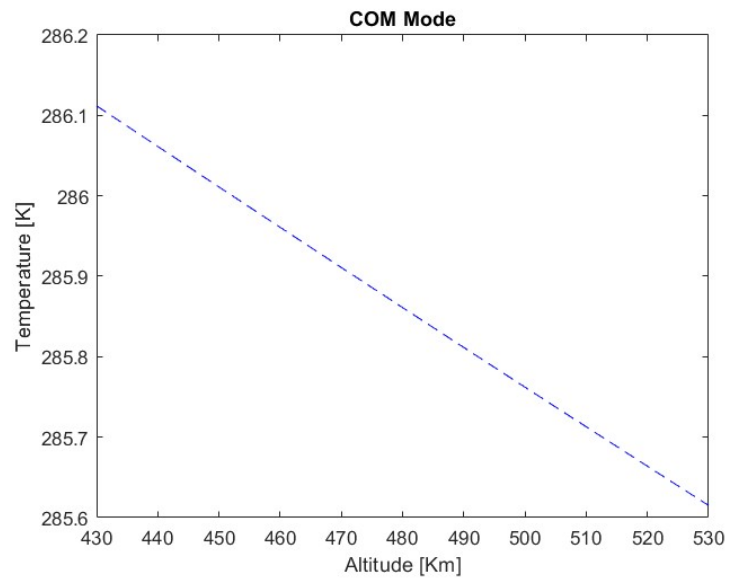Figure 26: Results obtained for COM Mode in cold case (240 K) and satellite's attitude of 97,33 degrees.

Figure 27: Results obtained for COM Mode in cold case (240 K) and satellite's attitude of 90 degrees.
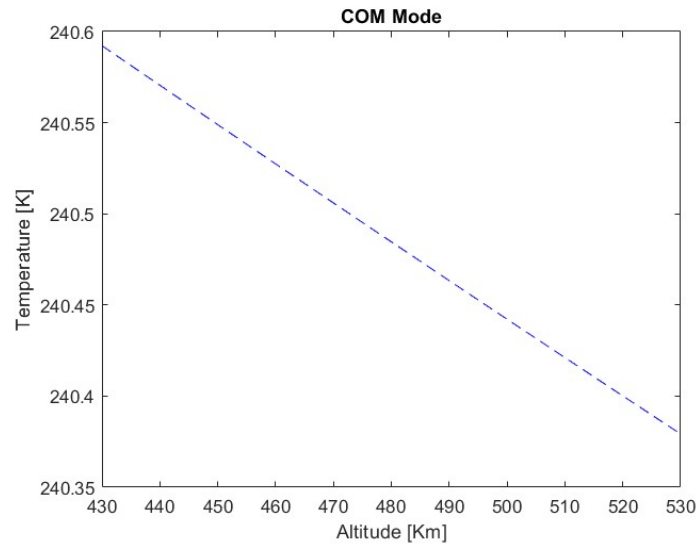
Figure 28: Results obtained for COM Mode in cold case (240 K) and satellite's attitude of 0 degrees.

For the cold case in Figure 26, Figure 27 and Figure 28, the same tendency as for the hot case can be observed. The only difference between the two cases is the values for the maximum and minimum temperatures achieved, which are a little bit lower in the cold case because the temperature of the Earth's surface is a little bit lower than in the cold case. It can also be seen that the maximum and minimum values of the temperature become closer and closer as the attitude of the satellite decreases, arriving at a point where the difference becomes so small (less than 0,25 K) that it can be said that the temperature is constant along the altitudes of the satellite that are studied.

3.1.2. CMEx Mode

In this operating mode, the power consumptions are exactly the same as in COM mode, but in this case the cameras and sensors are on, so the power consumption is higher than in COM mode, as it can be seen in Table 2. The results for this mode, for the hot and cold case and for each one of the attitudes of the satellite can be seen in the following figures.
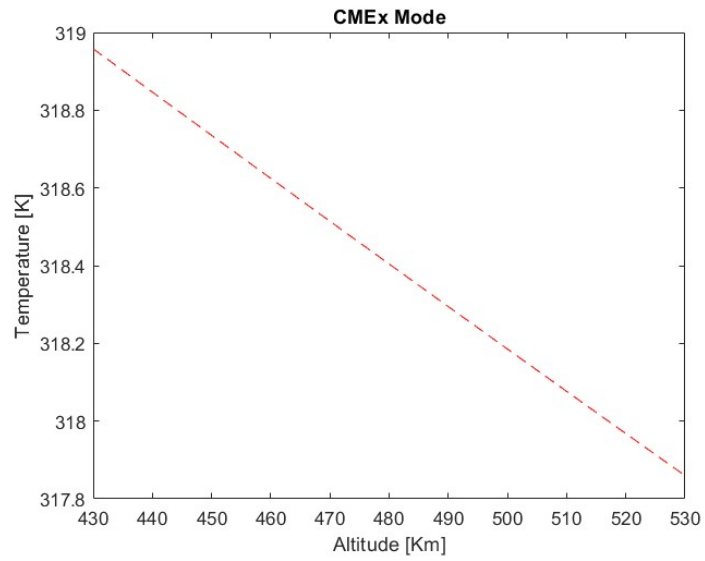
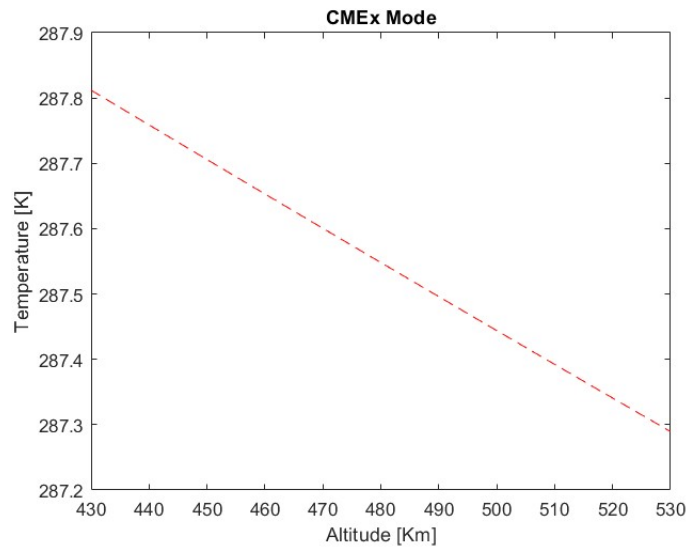Figure 29: Results obtained for CMEx Mode in hot case (260 K) and satellite's attitude of 97,33 degrees.

Figure 30: Results obtained for CMEx Mode in hot case (260 K) and satellite's attitude of 90 degrees.
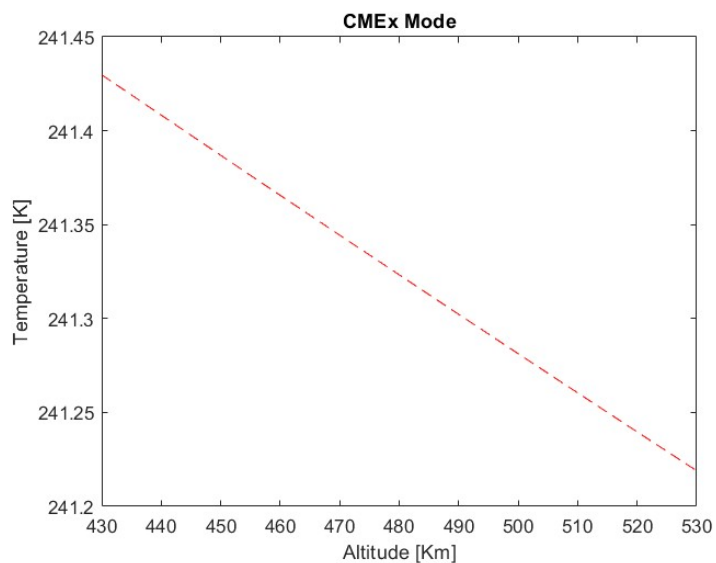
Figure 31: Results obtained for CMEx Mode in hot case (260 K) and satellite's attitude of 0 degrees.

In Figure 29, Figure 30 and Figure 31 it can be observed exactly the same tendency as in COM Mode, but in this case the values are a little bit higher than in COM Mode because the power consumed in CMEx Mode is higher than in COM Mode as it can be observed in Table 2. The same conclusions as for the COM Mode can be derived from the results obtained in CMEx Mode.
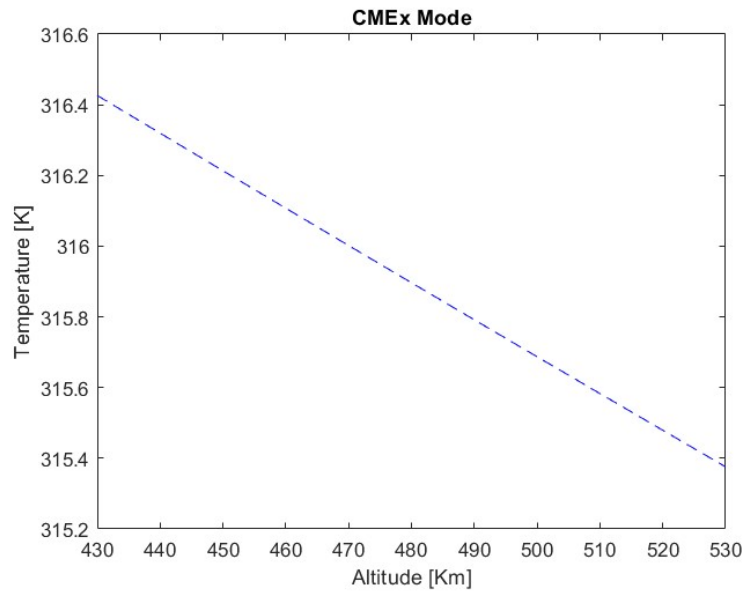

Figure 32: Results obtained for CMEx Mode in cold case (240 K) and satellite's attitude of 97,33 degrees.
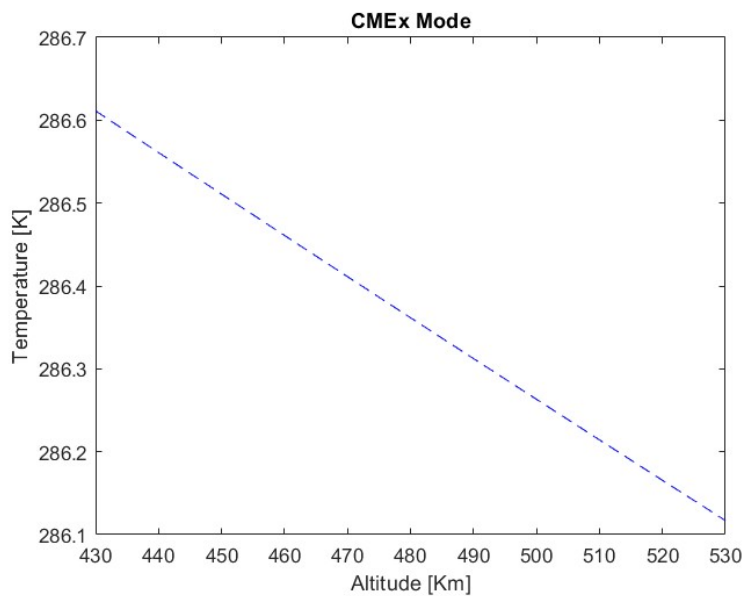

Figure 33: Results obtained for CMEx Mode in cold case (240 K) and satellite's attitude of 90 degrees.
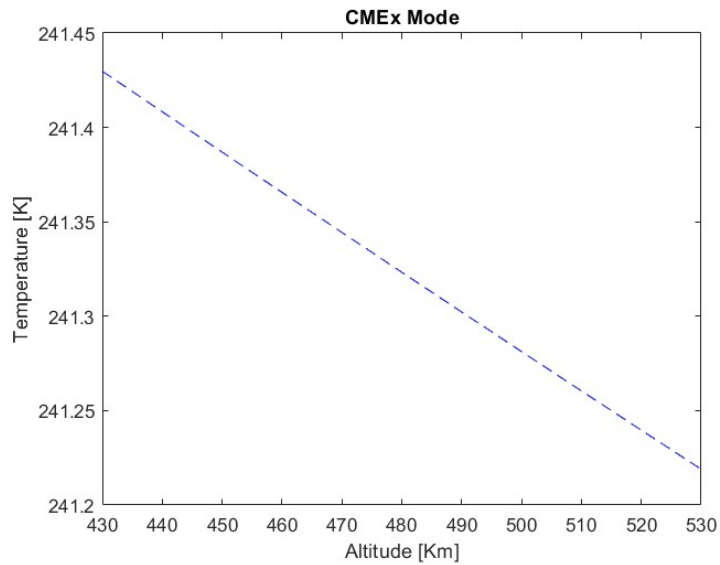
Figure 34: Results obtained for CMEx Mode in cold case (240 K) and satellite's attitude of 0 degrees.

From Figure 32, Figure 33 and Figure 34 can be observed that the tendency is exactly the same as in the previous cases, but the values are higher than in the cold case of COM Mode. This is because the power consumed by CMEx Mode is higher than in COM Mode, as stated in Table 2.

3.1.3. COM_CMEx Mode

During this mode, all the components that are working on COM mode are on, and also the ones that work in CMEx mode, so all the sensors and cameras are working, and also the transceiver for the communications. In short, this is the same case as in the CMEx mode, with the results being the following ones.
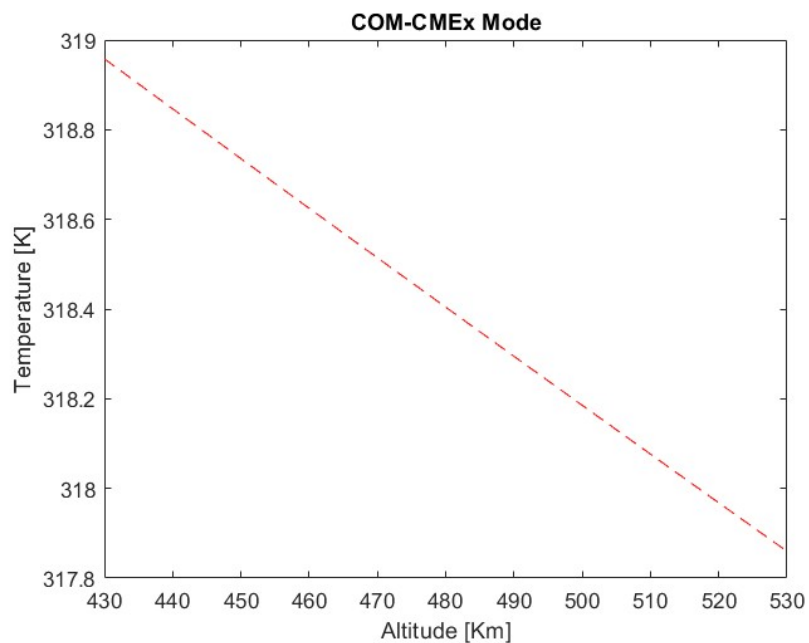

Figure 35: Results obtained for COM_CMEx Mode in hot case (260 K) and satellite's attitude of 97,33 degrees.
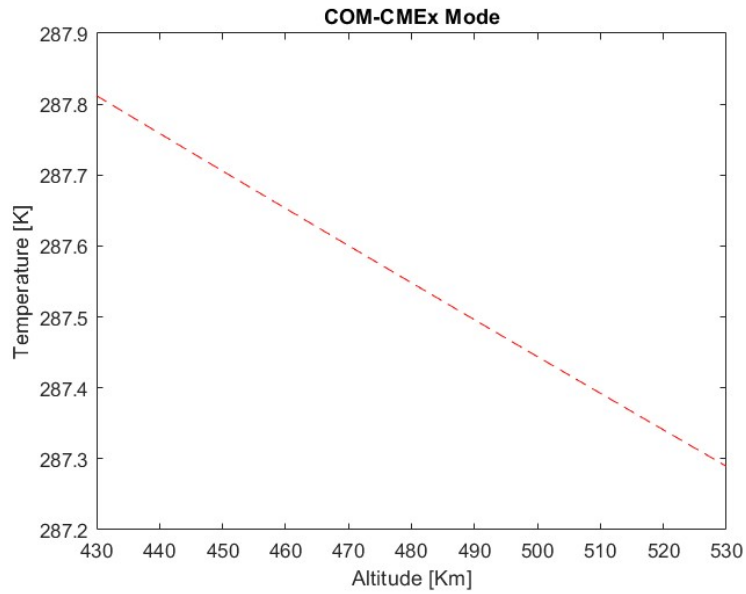
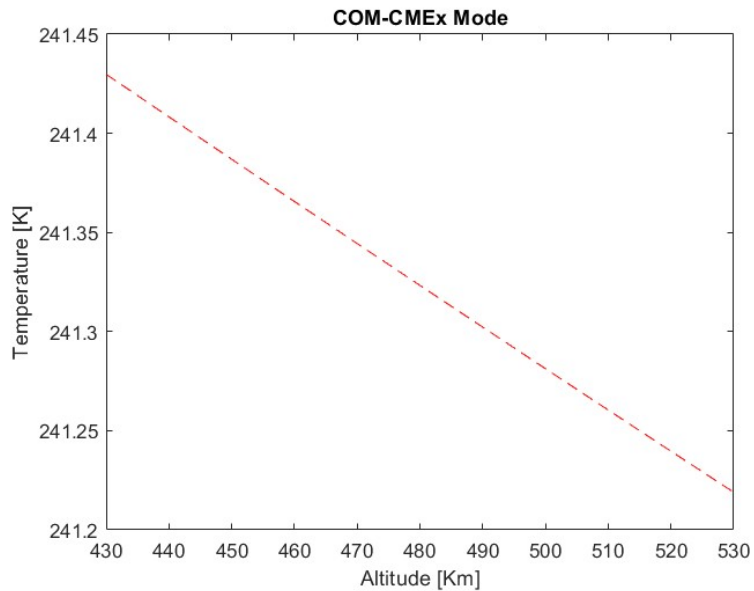Figure 36: Results obtained for COM_CMEx Mode in hot case (260 K) and satellite's attitude of 90 degrees.

Figure 37: Results obtained for COM_CMEx Mode in hot case (260 K) and satellite's attitude of 0 degrees.

As it can be seen in Figure 35, Figure 36 and Figure 37, the tendency is exactly the same as in the previous cases. Another thing that can be observed is that the values of the temperature are exactly the same as for the hot case in CMEx Mode. This is because the power consumed in CMEx and in COM_CMEx are the same, so the temperature of the surface of the satellite must be the same, as can be seen in Figure 35, Figure 36 and Figure 37.
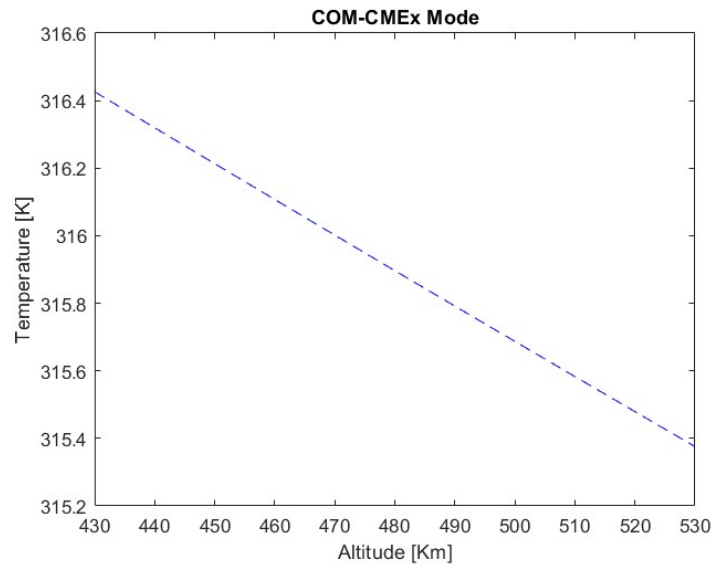
Figure 38: Results obtained for COM_CMEx Mode in cold case (240 K) and satellite's attitude of 97,33 degrees.
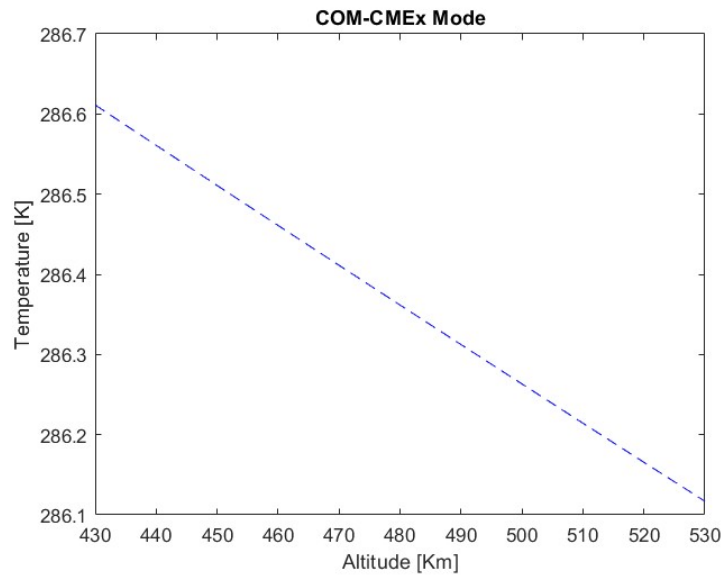

Figure 39: Results obtained for COM_CMEx Mode in cold case (240 K) and satellite's attitude of 90 degrees.
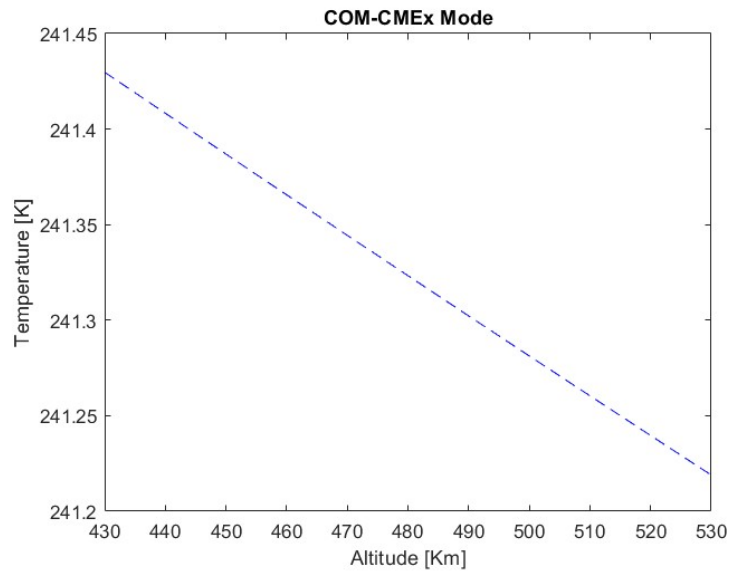
Figure 40: Results obtained for COM_CMEx Mode in cold case (240 K) and satellite's attitude of 0 degrees.

In Figure 38, Figure 39 and Figure 40 the tendency that can be observed is exactly the same as in all the previous cases, and the values for the surface's temperature in COM_CMEx Mode are exactly the same as in the cold case for CMEx Mode, because the power consumed by the satellite in these two modes is the same, as can be seen in Table 2.

3.1.4. MAX_CHARGE Mode

During MAX_CHARGE mode, TRACE satellite faces to the Sun so it can receive the solar energy needed to charge its batteries more rapidly and efficiently. During this mode, the satellite does not use its sensors or cameras, only utilizes its transceiver to communicate, so this is the reason why the power used by TRACE satellite is exactly the same as in COM (Communication) mode. The results for this operating mode are presented in the following.
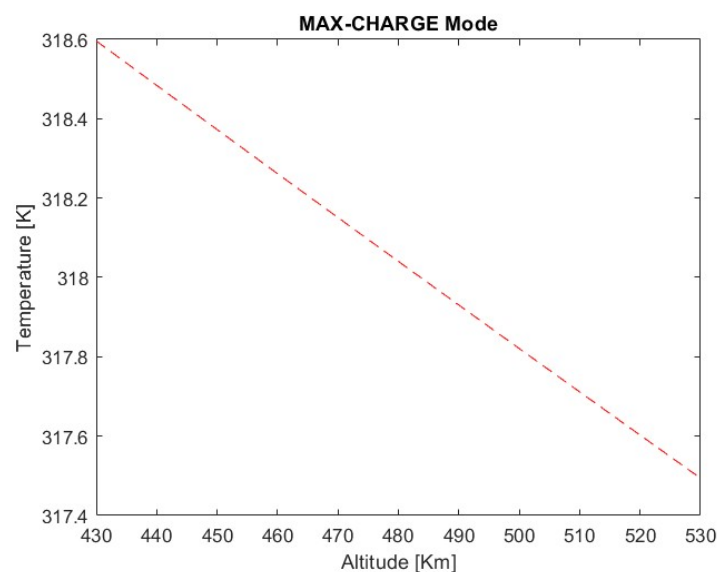
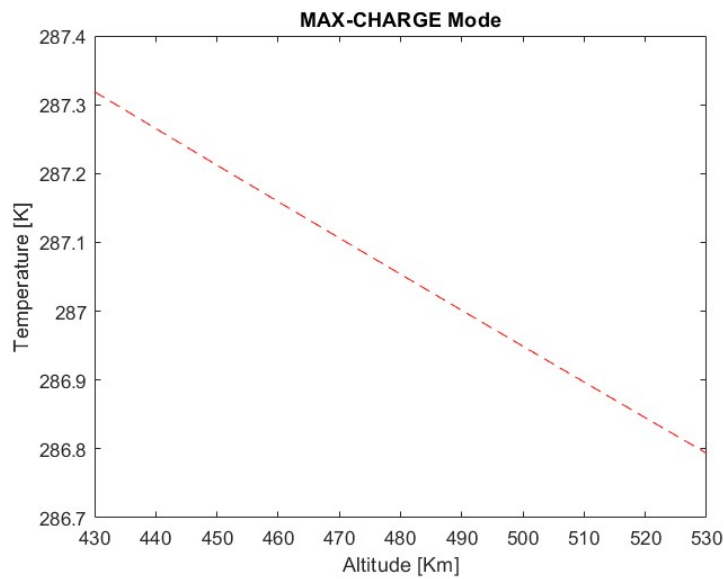Figure 41: Results obtained for MAX_CHARGE Mode in hot case (260 K) and satellite's attitude of 97,33 degrees.

Figure 42: Results obtained for MAX_CHARGE Mode in hot case (260 K) and satellite's attitude of 90 degrees.

Figure 43: Results obtained for MAX_CHARGE Mode in hot case (260 K) and satellite's attitude of 0 degrees.

The conclusions that can be drawn from Figure 41, Figure 42 and Figure 43 are that the tendency observed in the results is the same as in the previous cases: a decrease in temperature with an increase in the satellite's altitude. The values of the surface's temperature that are obtained are the same values as for COM Mode, but are slightly lower than in CMEx or COM_CMEx Modes because the power consumed in MAX_CHARGE Mode is the same as in COM Mode but lower than in CMEx or COM_CMEx Mode, as seen in Table 2.

Figure 44: Results obtained for MAX_CHARGE Mode in cold case (240 K) and satellite's attitude of 97,33 degrees.

Figure 45: Results obtained for MAX_CHARGE Mode in cold case (240 K) and satellite's attitude of 90 degrees.
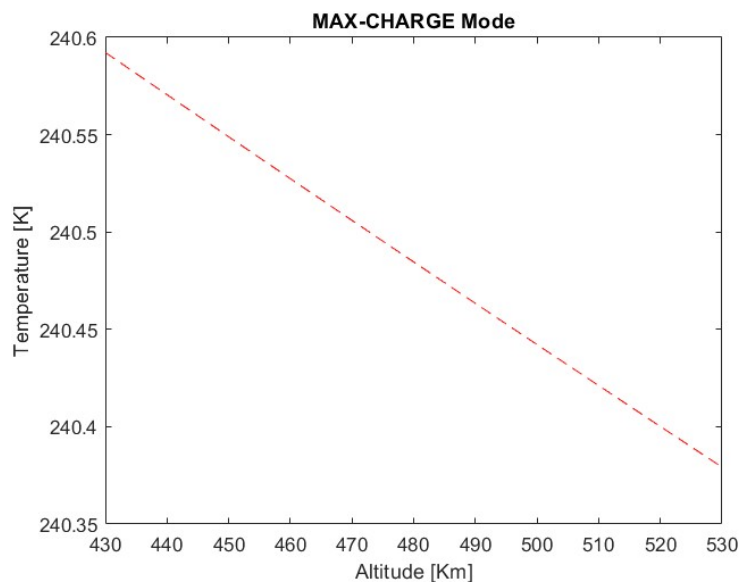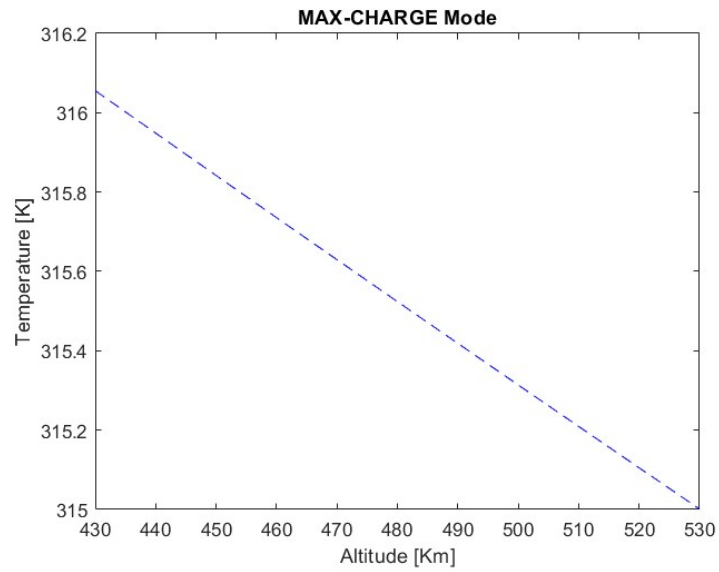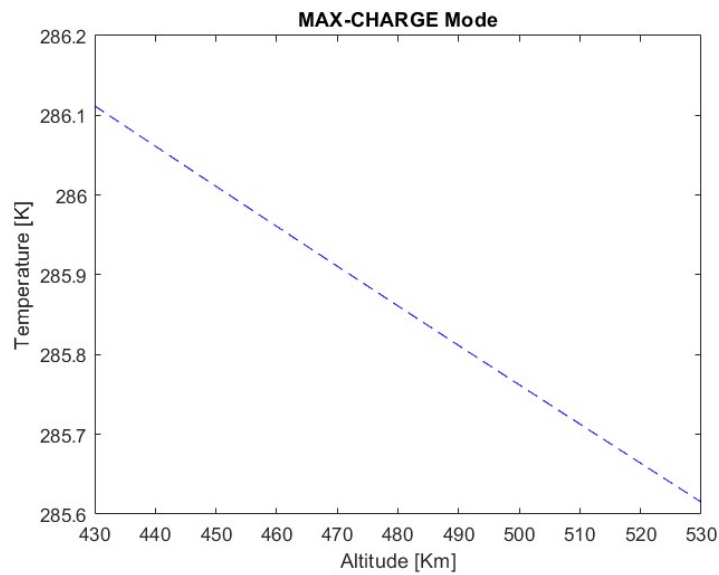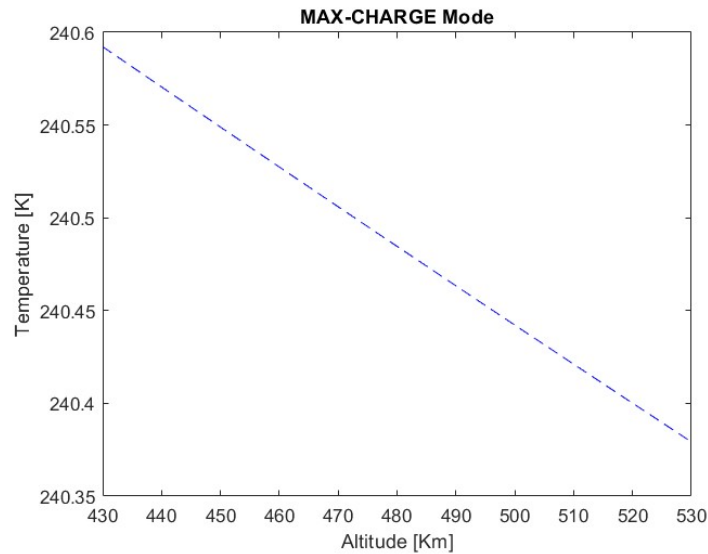
Figure 46: Results obtained for MAX_CHARGE Mode in cold case (240 K) and satellite's attitude of 0 degrees.

From Figure 44, Figure 45 and Figure 46 the conclusions that can be drawn are that the tendency (decrease in temperature with an increase in altitude) is exactly the same as in all the previous cases, and that the values for the surface's temperature of the satellite are the same as in COM Mode (because both modes, COM and MAX_CHARGE consume the same amount of power), but this temperature is a little bit lower than in CMEx or COM_CMEx Modes for the same reason, a lower power consumption and thus a lower heat radiation as can be seen in Table 2.

3.2. Transient Thermal Analysis Results

The results obtained for the transient analysis are obtained using the procedure described in section 2.2. For the results in this section, they are presented following all the limitations explained in section 2.2, so the only variable that exists in these results is the albedo, that varies from 0.3 to 0.8 to try to observe its influence in the surface's temperature of TRACE satellite. One comment that needs to be made is that the results obtained for the COM mode and for the MAX_CHARGE mode are exactly the same due to the same power as it can be seen in Table 2, as well as the results for the CMEx and COM_CMEx modes, which are also equal. Because of this pattern, only the results for COM and CMEx modes are presented.

Another clarification that needs to be made is that the values are obtained for the lumps on each face, as it can be seen in Figure 20. And finally, the central lump (node 1 in Figure 20) is studied independently of the other lumps.

3.2.1. Transient COM Results

The results obtained for the COM operating mode are presented below.

Figure 47: Faces Temperatures for transient COM (and MAX_CHARGE) Mode and albedo coefficient of 0,3.

Figure 48: Faces Temperatures for transient COM (and MAX_CHARGE) Mode and albedo coefficient of 0,4.

Figure 49: Faces Temperatures for transient COM (and MAX_CHARGE) Mode and albedo coefficient of 0,5.
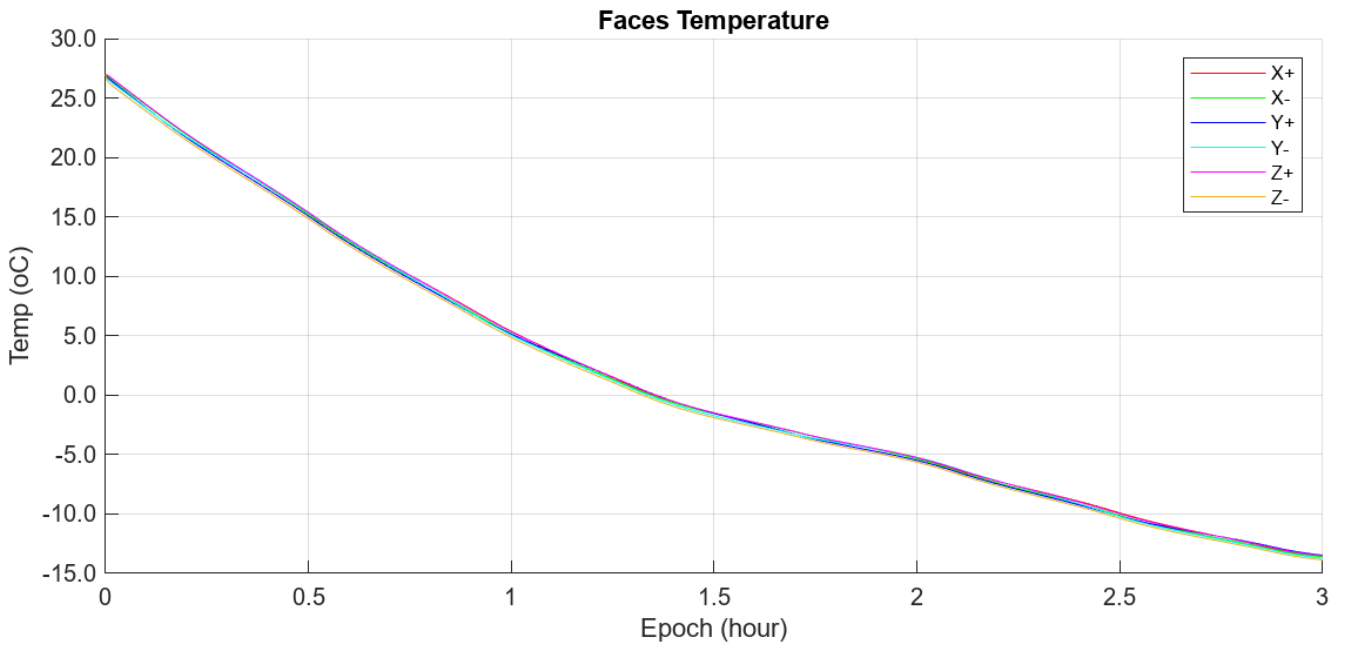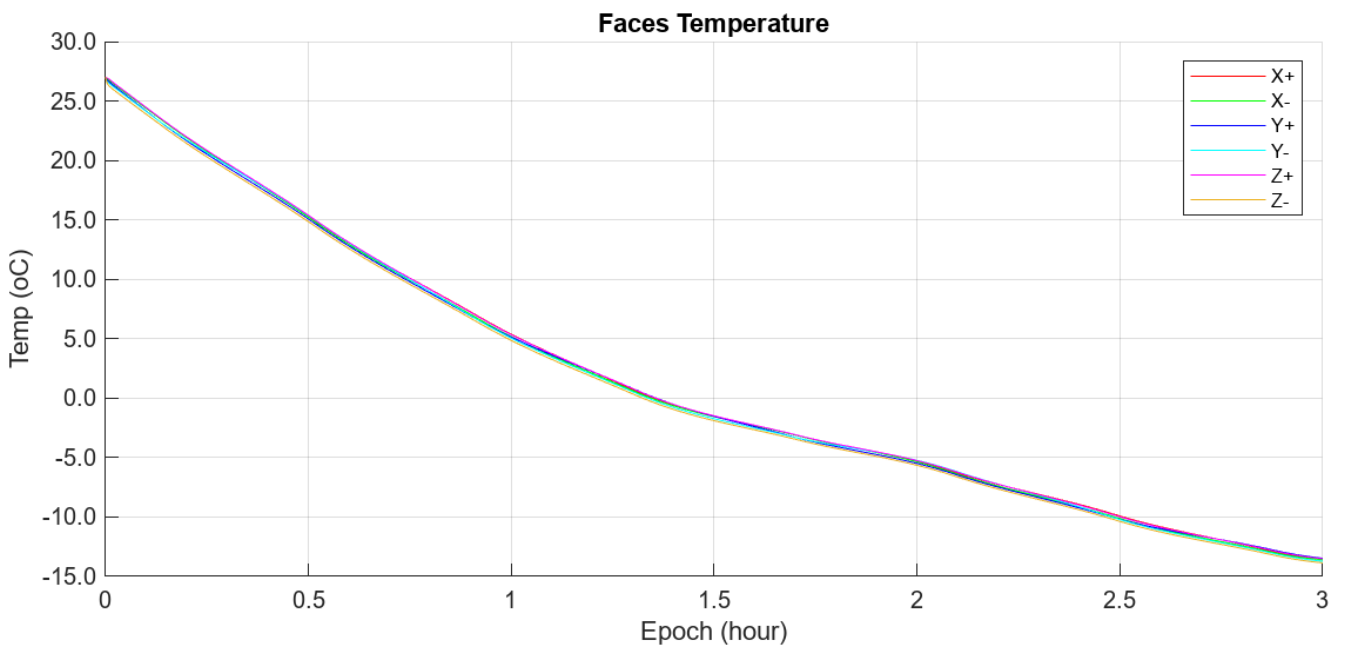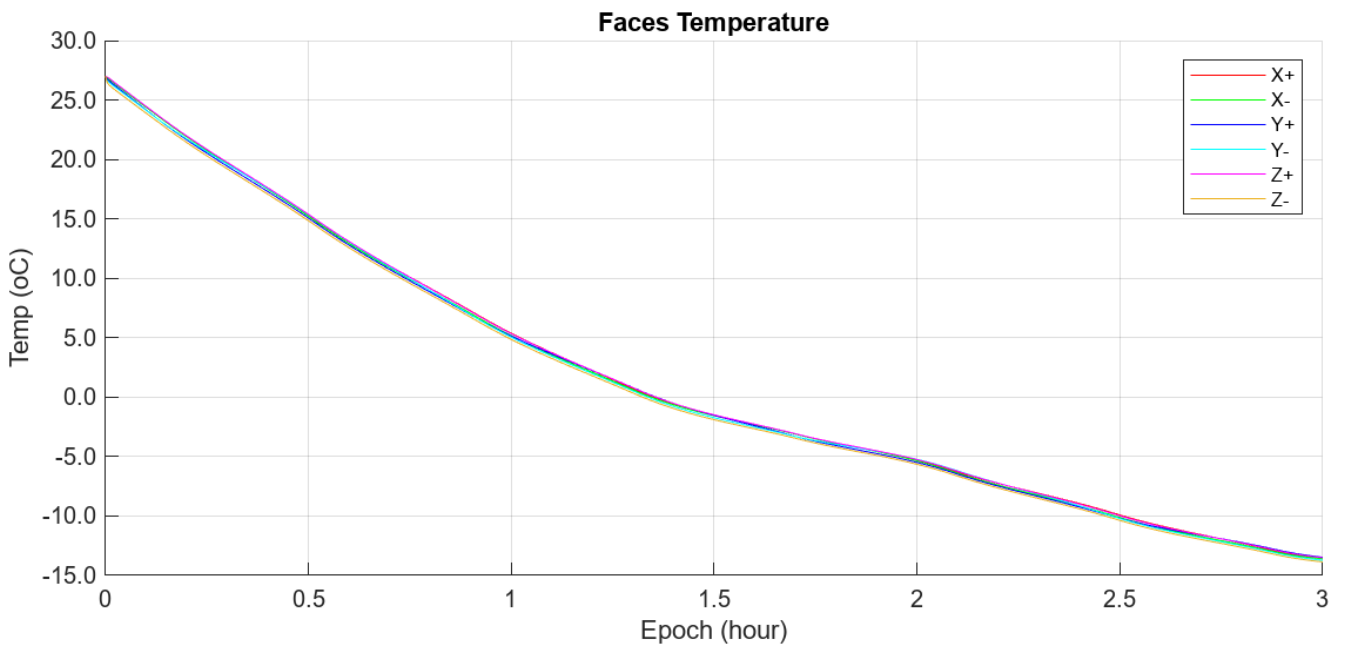

Figure 50: Faces Temperatures for transient COM (and MAX_CHARGE) Mode and albedo coefficient of 0,6.
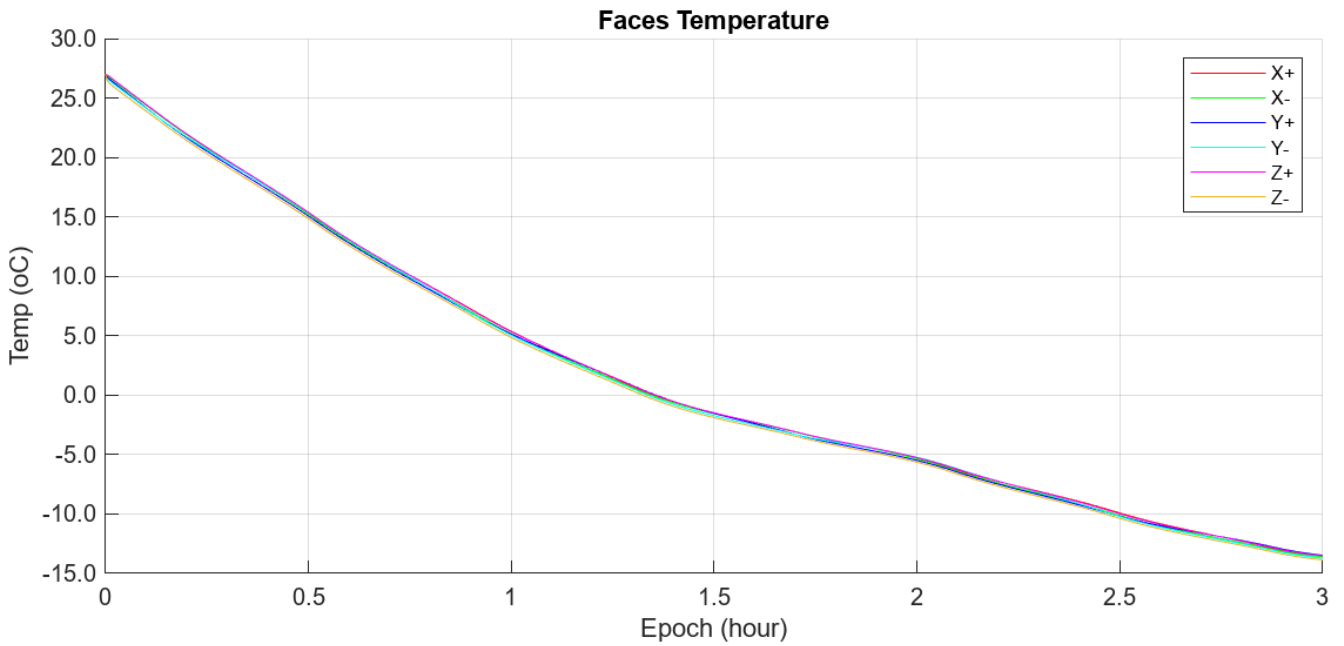
Figure 51: Faces Temperatures for transient COM (and MAX_CHARGE) Mode and albedo coefficient of 0,7.
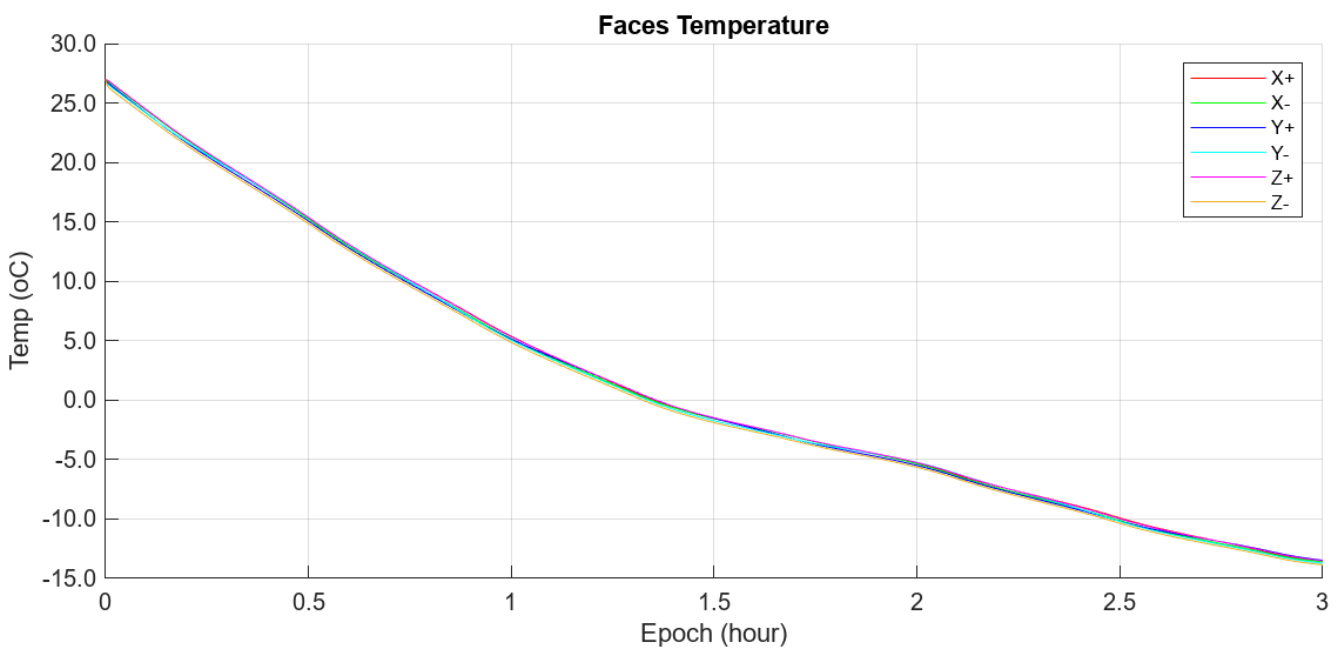
Figure 52: Faces Temperatures for transient COM (and MAX_CHARGE) Mode and albedo coefficient of 0,8.

From Figure 47, Figure 48, Figure 49, Figure 50, Figure 51 and Figure 52 it can be deduced that the temperature decreases while TRACE satellite travels through its orbit. Another conclusion is that the temperatures of each one of the faces of the satellite are practically the same, and temperatures decrease in an exponential way, differently as in the steady study, which was more as a lineal decrease. Finally, it can be seen that the decrease is much more pronounced than in the steady study.

Figure 53: Internal Temperature for transient COM (and MAX_CHARGE) Mode and albedo coefficient of 0,3.

Figure 54: Internal Temperature for transient COM (and MAX_CHARGE) Mode and albedo coefficient of 0,4.

Figure 55: Internal Temperature for transient COM (and MAX_CHARGE) Mode and albedo coefficient of 0,5.

Figure 56: Internal Temperature for transient COM (and MAX_CHARGE) Mode and albedo coefficient of 0,6.
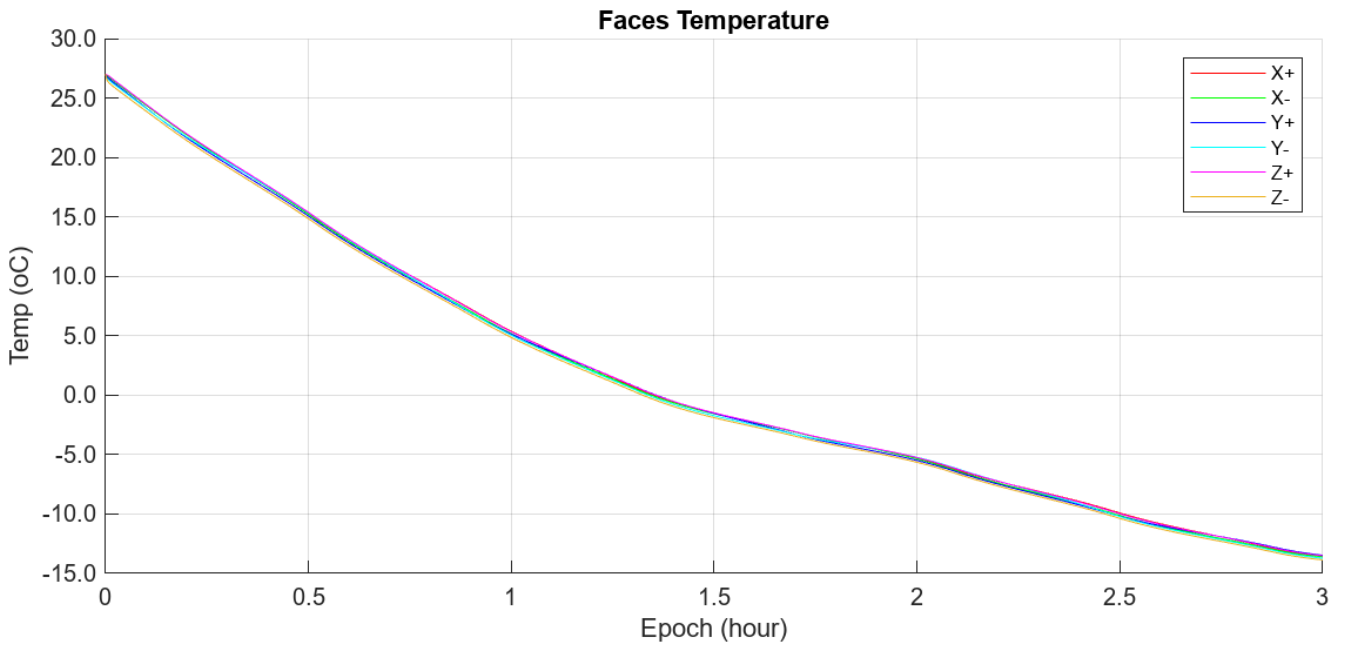
Figure 57: Internal Temperature for transient COM (and MAX_CHARGE) Mode and albedo coefficient of 0,7.

Figure 58: Internal Temperature for transient COM (and MAX_CHARGE) Mode and albedo coefficient of 0,8.

From Figure 53, Figure 54, Figure 55, Figure 56, Figure 57 and Figure 58 the same conclusions as for the faces' temperatures can be drawn. The decrease is more exponential than in the steady study and also difference between the maximum and minimum temperatures of the surface is much higher than in the steady study.

3.2.2. Transient CMEx Results

As for the COM (and MAX_CHARGE) modes has been made, in the following, the results for the CMEx operating mode are presented.
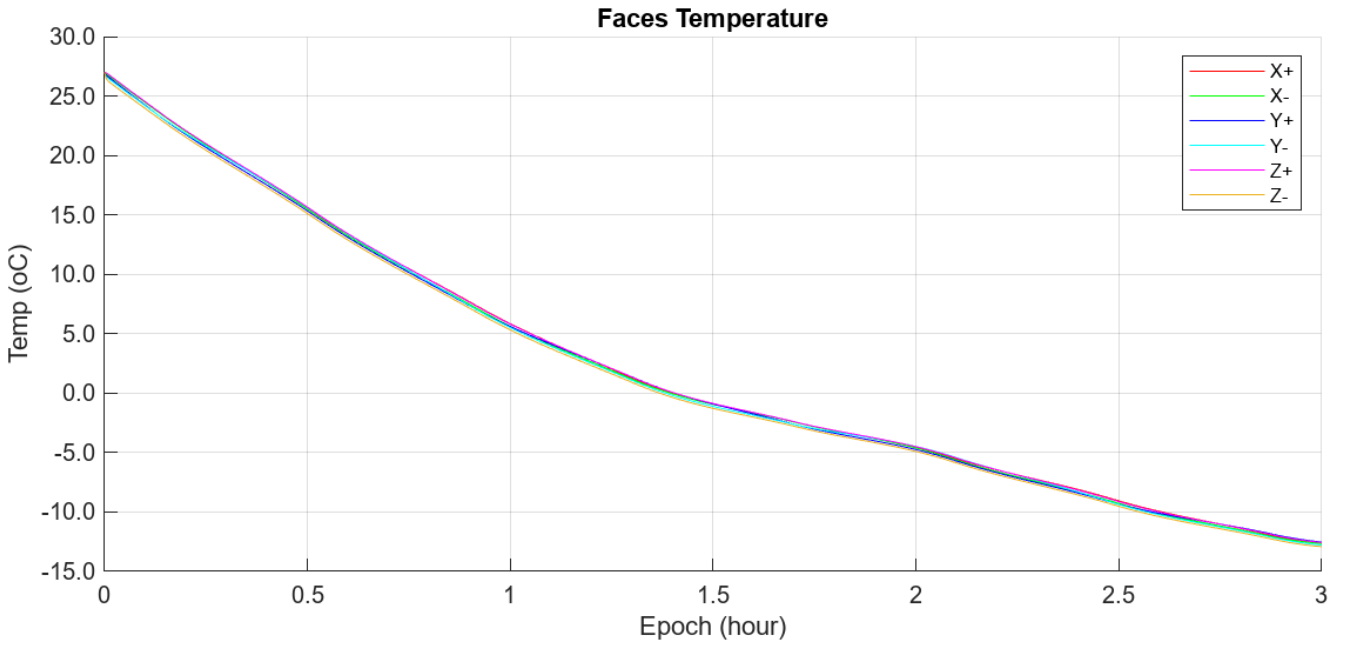
Figure 59: Faces Temperatures for transient CMEx (and COM_CMEx) Mode and albedo coefficient of 0,3.
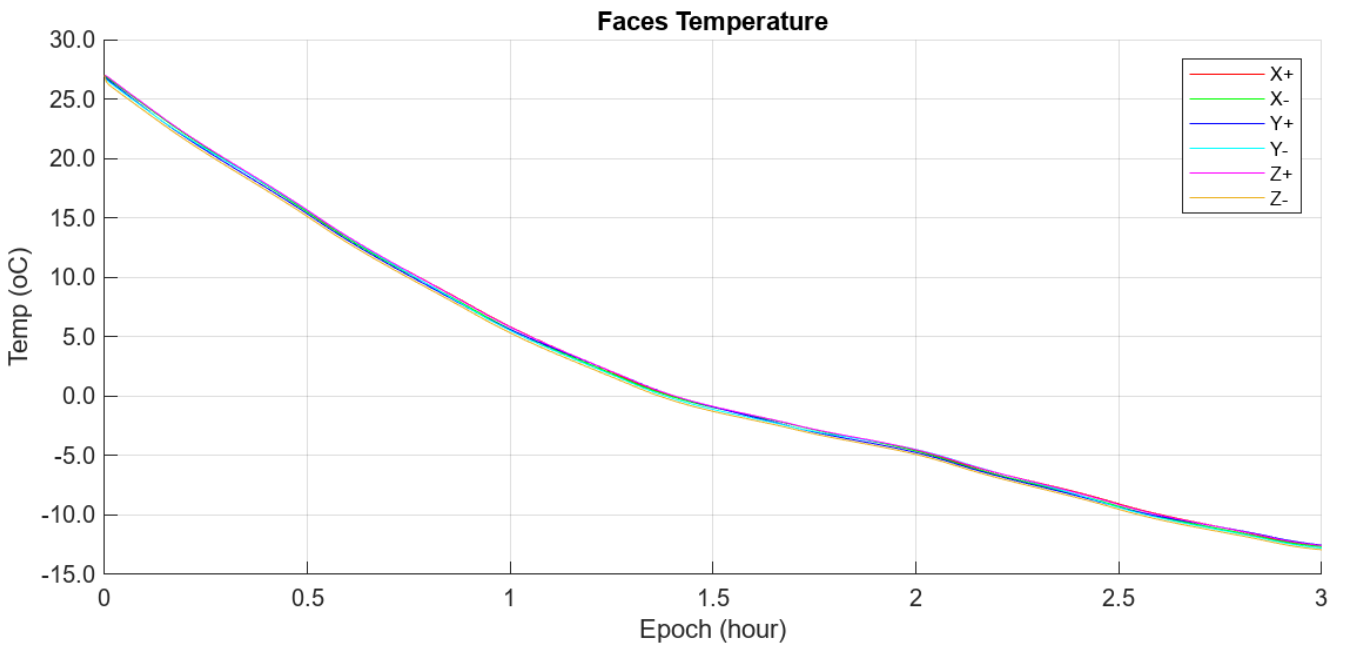
Figure 60: Faces Temperatures for transient CMEx (and COM_CMEx) Mode and albedo coefficient of 0,4.
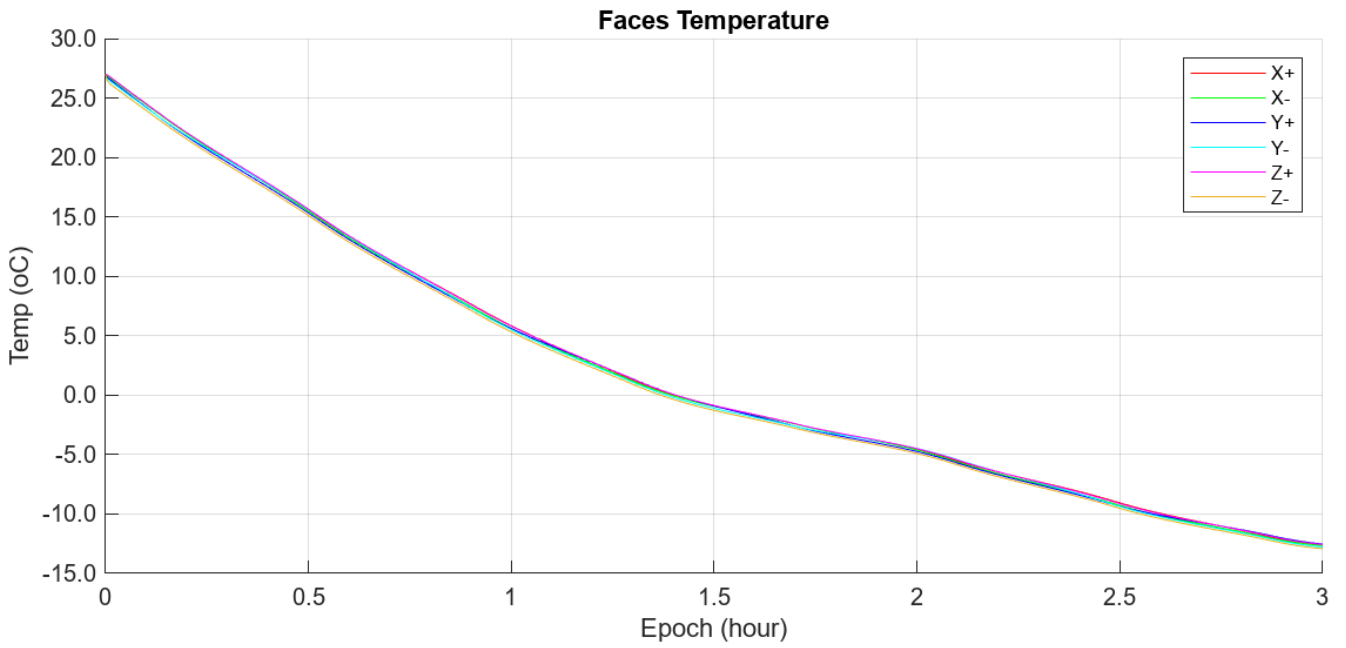
Figure 61: Faces Temperatures for transient CMEx (and COM_CMEx) Mode and albedo coefficient of 0,5.
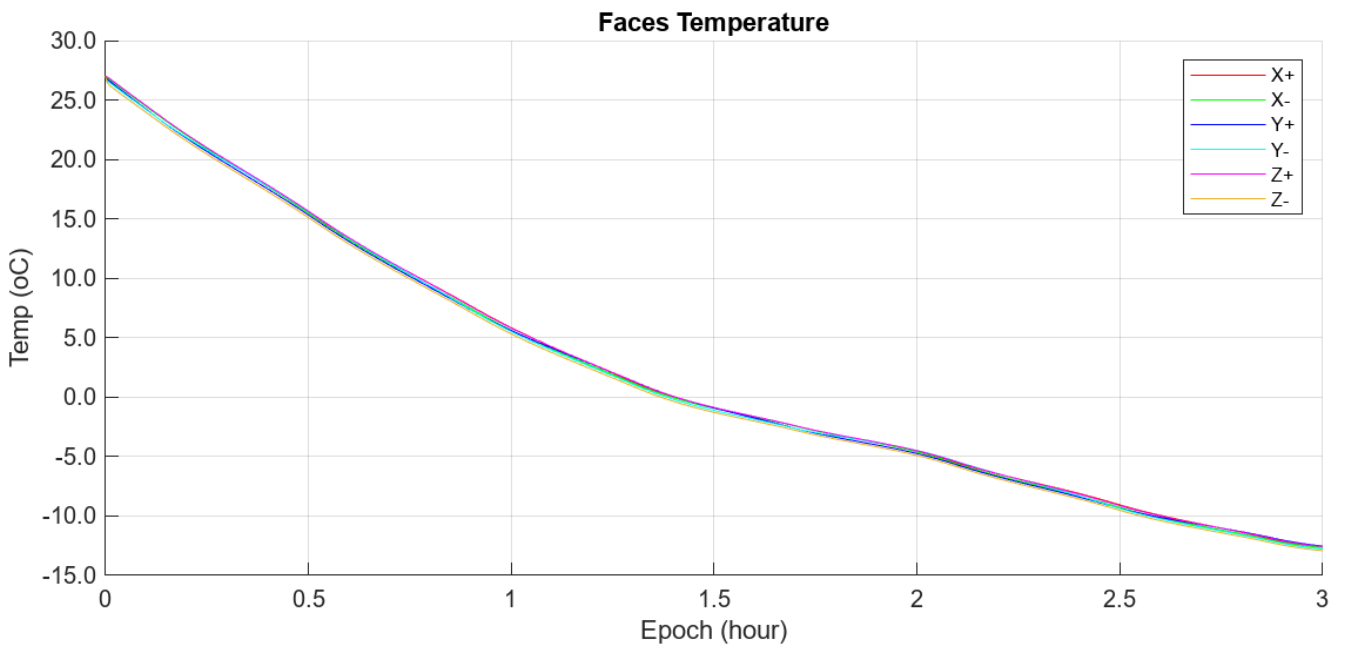
Figure 62: Faces Temperatures for transient CMEx (and COM_CMEx) Mode and albedo coefficient of 0,6.
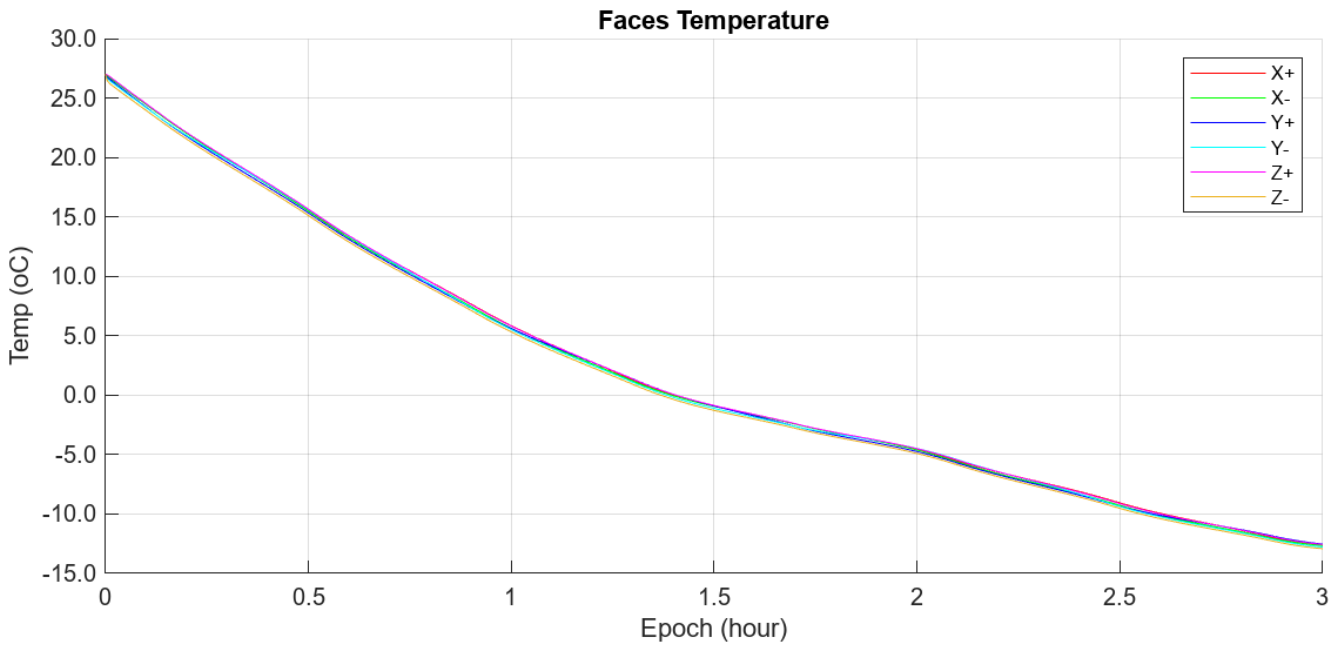
Figure 63: Faces Temperatures for transient CMEx (and COM_CMEx) Mode and albedo coefficient of 0,7.

Figure 64: Faces Temperatures for transient CMEx (and COM_CMEx) Mode and albedo coefficient of 0,8.

From Figure 59, Figure 60, Figure 61, Figure 62, Figure 63 and Figure 64, the same conclusions can be drawn as for the COM and MAX_CHARGE working modes, except in this case, the values of the temperature are a little bit higher because the power consumption, and thus the heat radiation, in CMEx and in COM_CMEx is a little bit higher, as shown in Table 2.
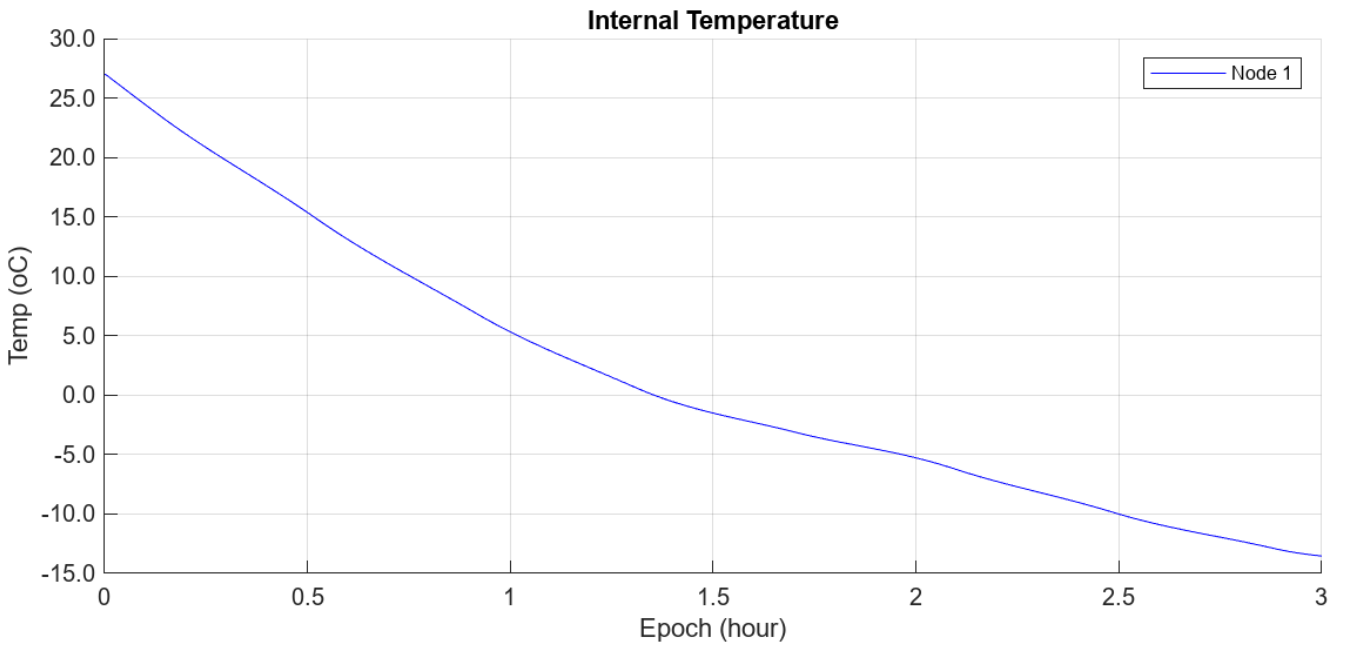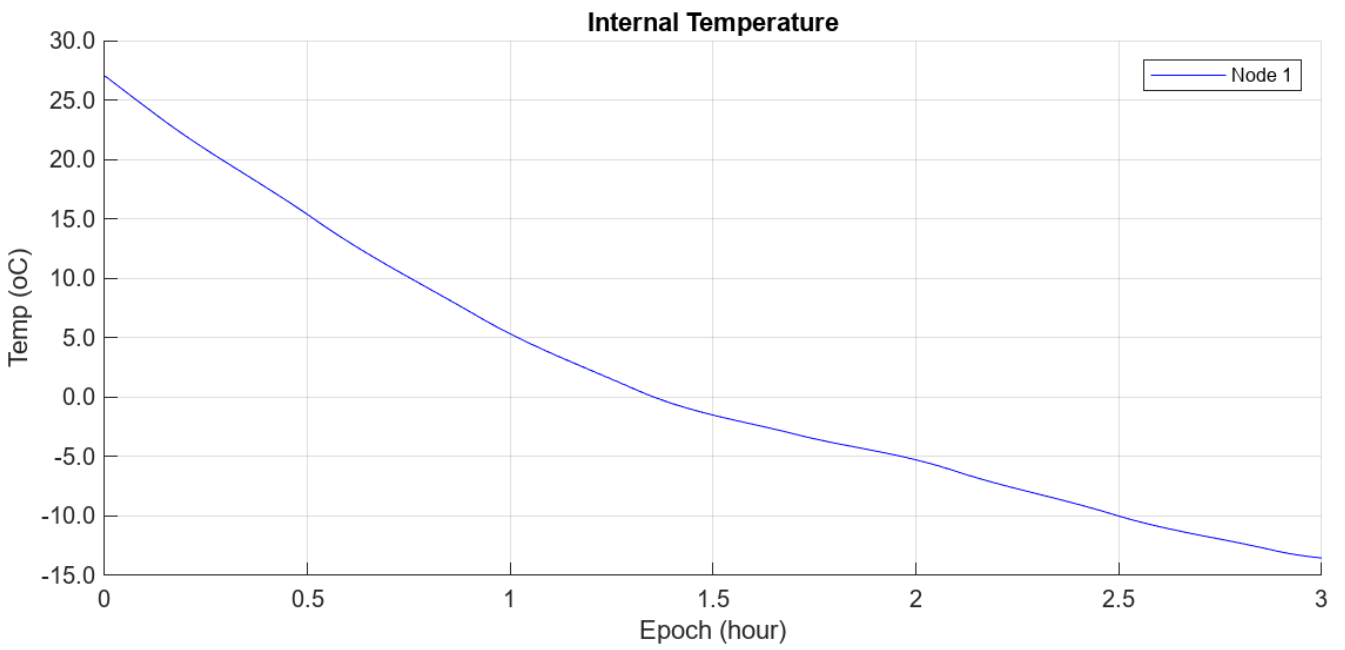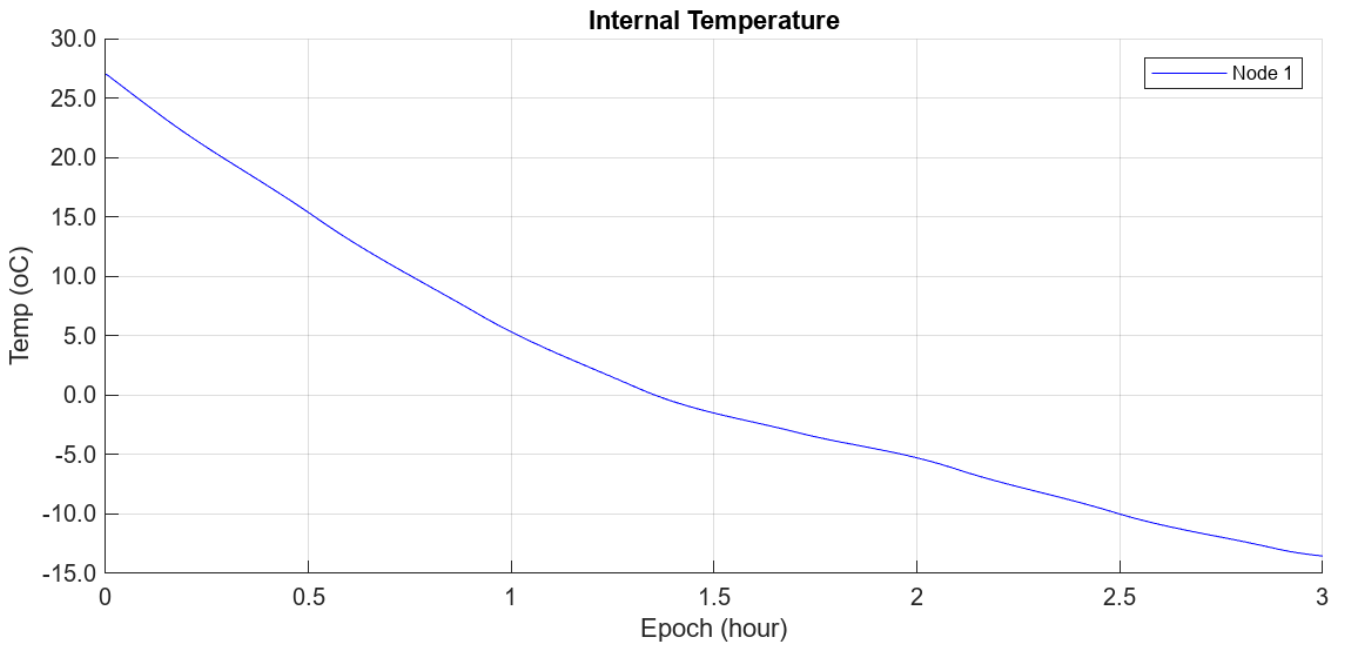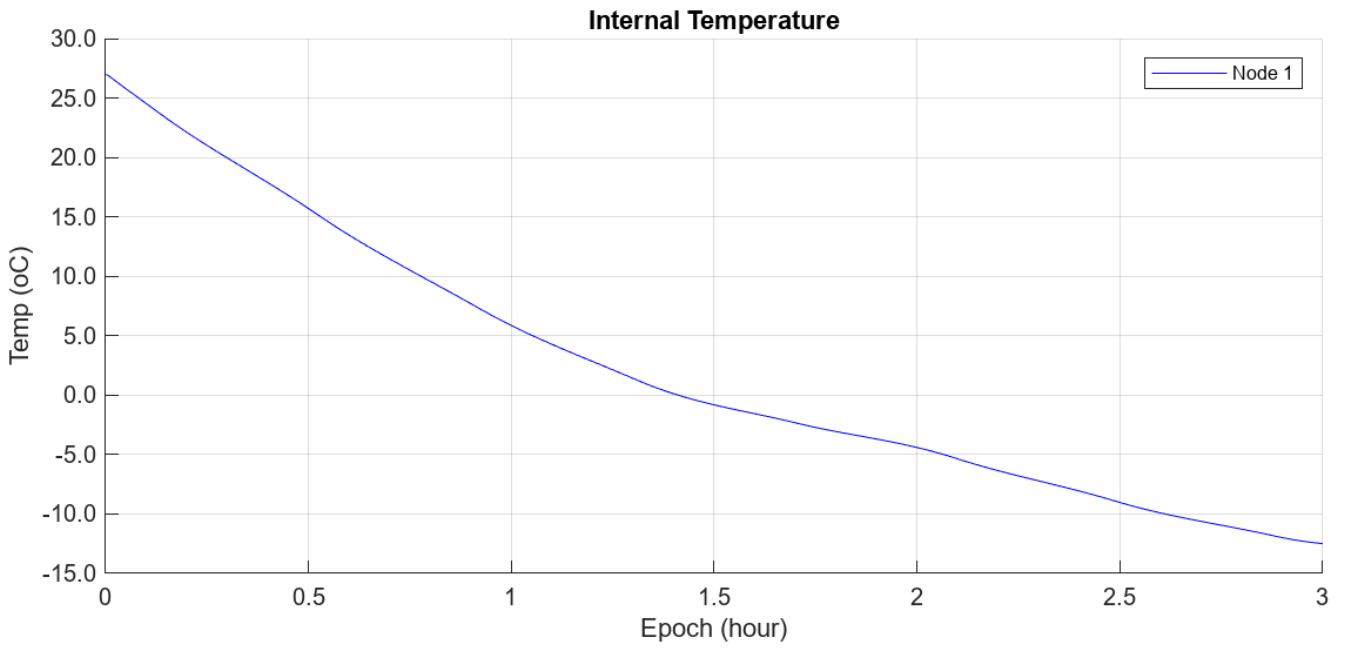
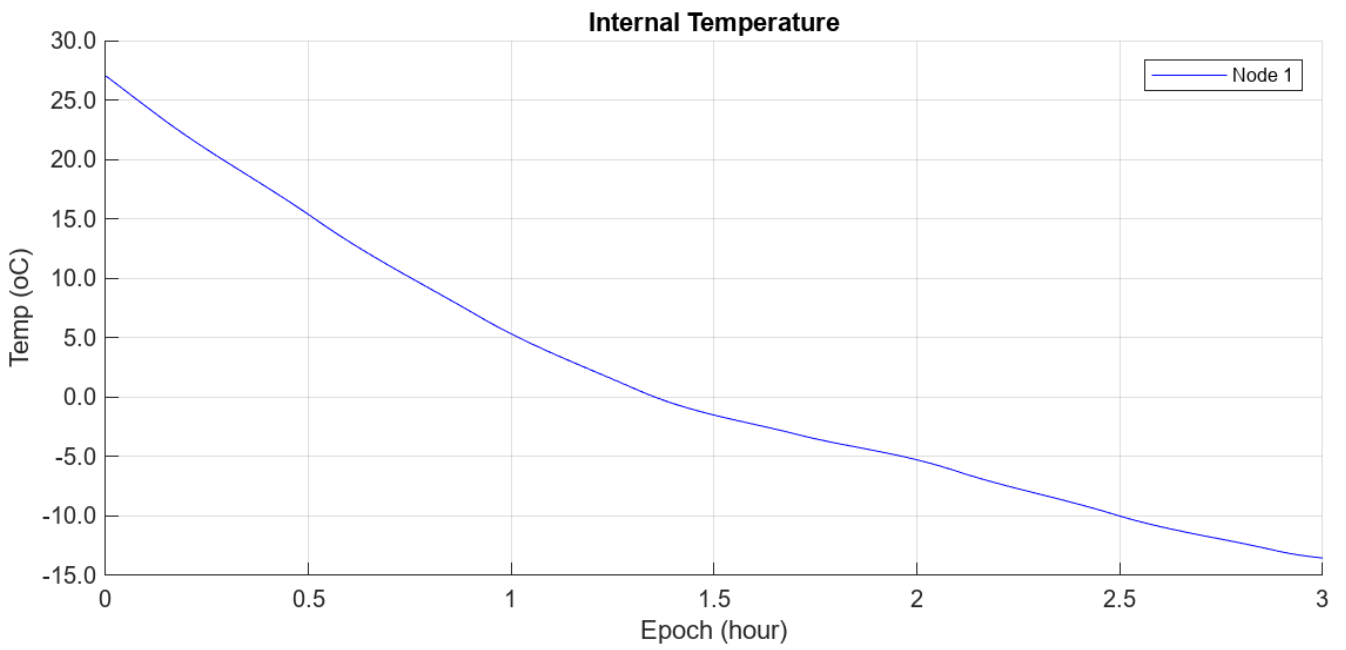Figure 65: Internal Temperature for transient CMEx (and COM_CMEx) Mode and albedo coefficient of 0,3.
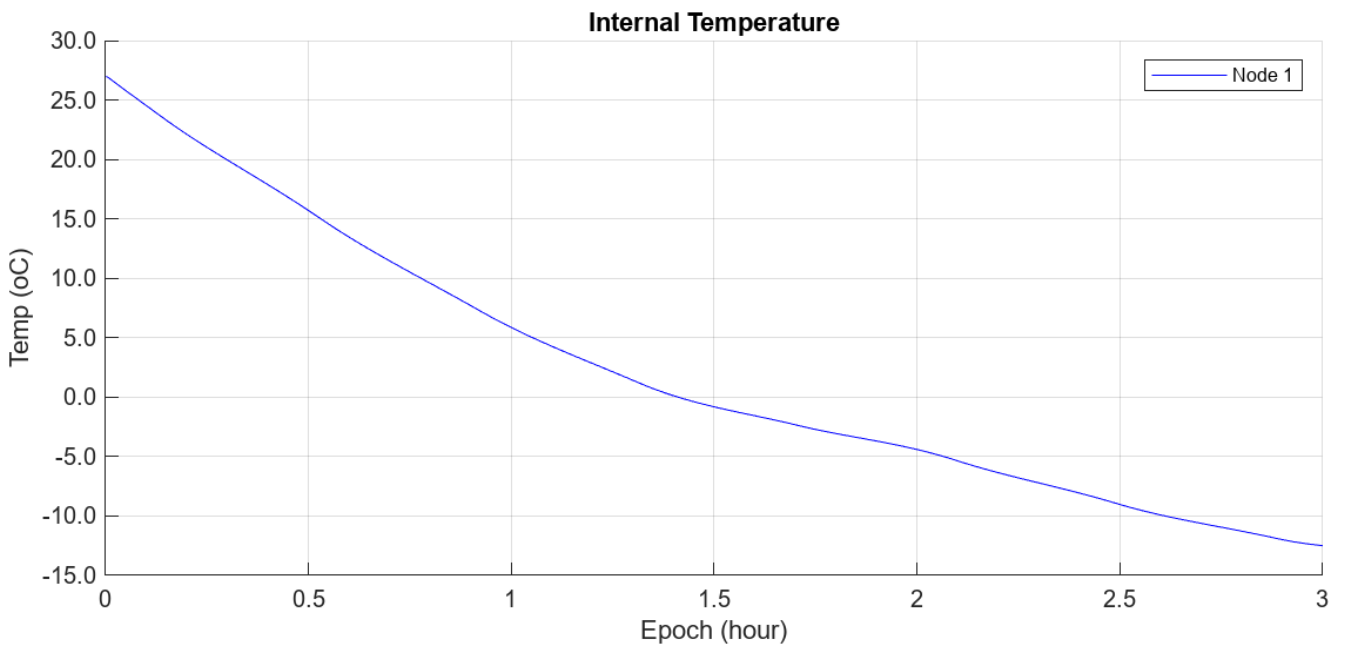
Figure 66: Internal Temperature for transient CMEx (and COM_CMEx) Mode and albedo coefficient of 0,4.
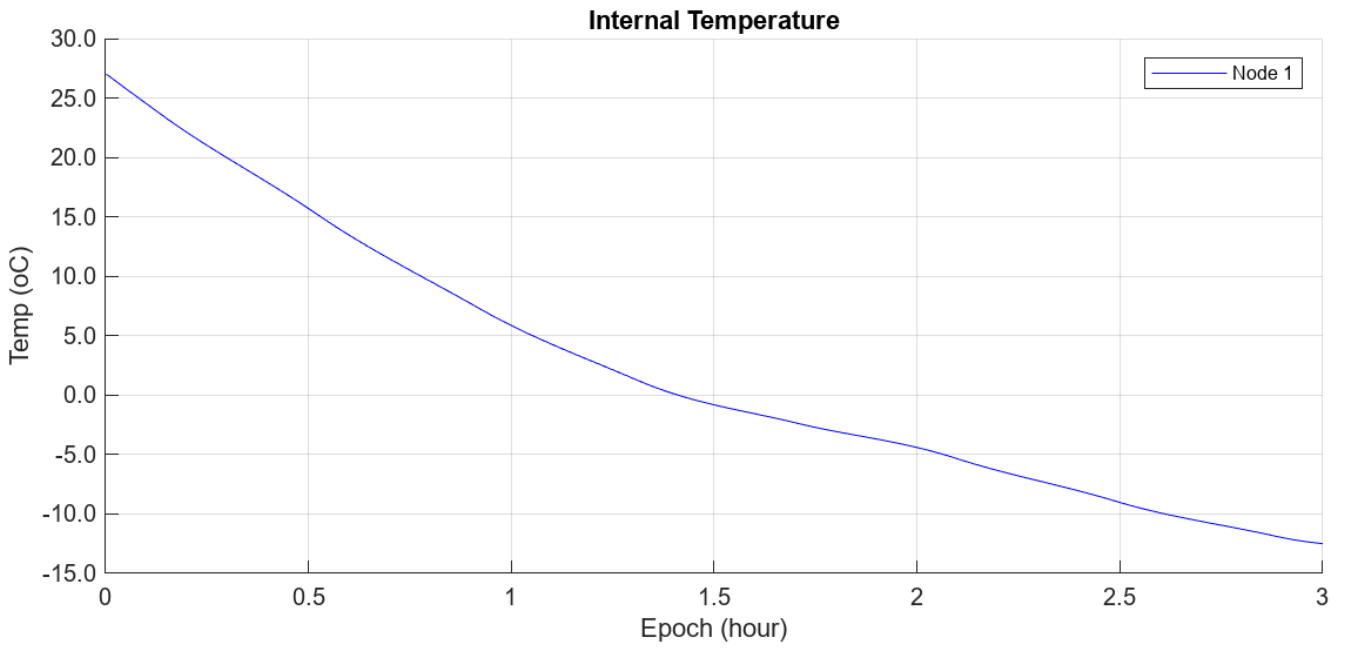
Figure 67: Internal Temperature for transient CMEx (and COM_CMEx) Mode and albedo coefficient of 0,5.
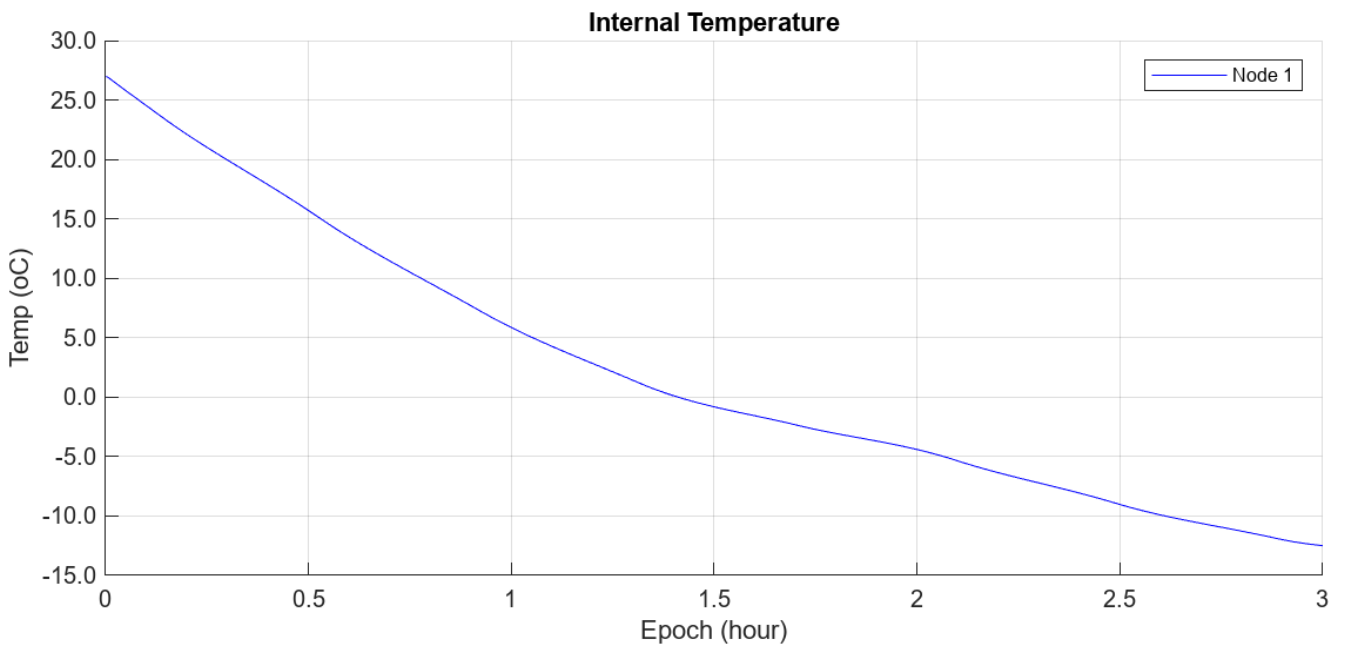
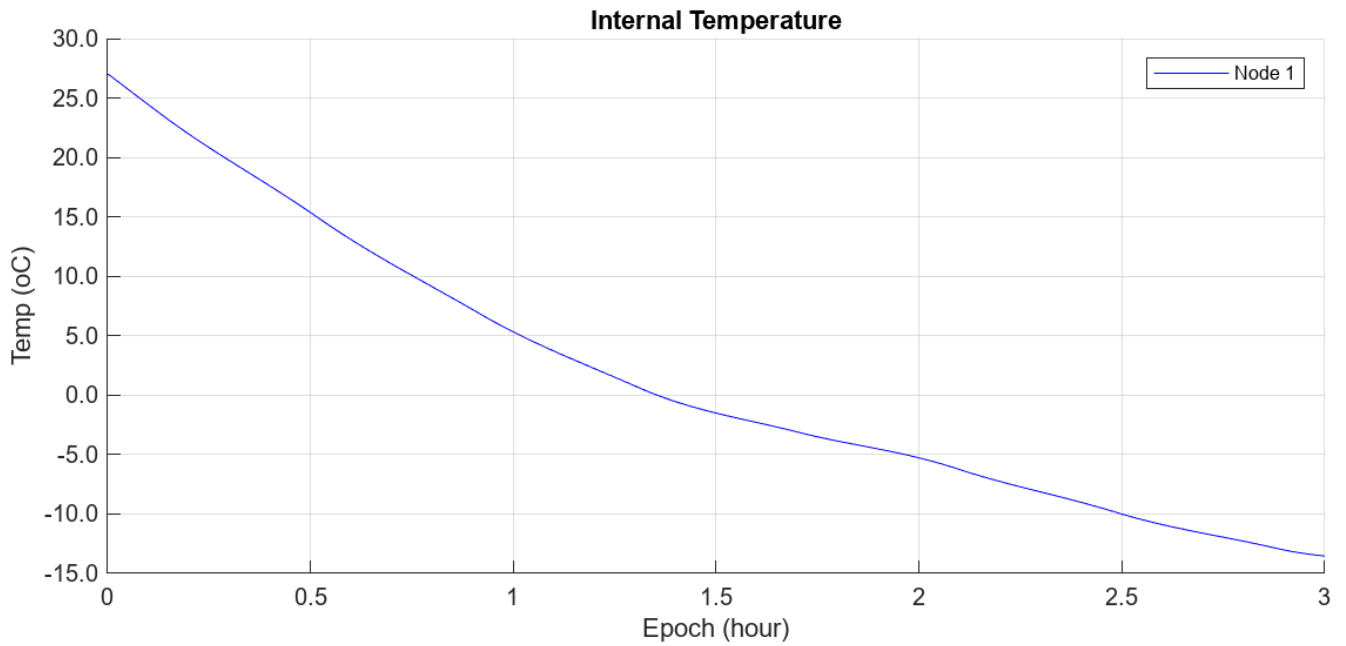Figure 68: Internal Temperature for transient CMEx (and COM_CMEx) Mode and albedo coefficient of 0,6.
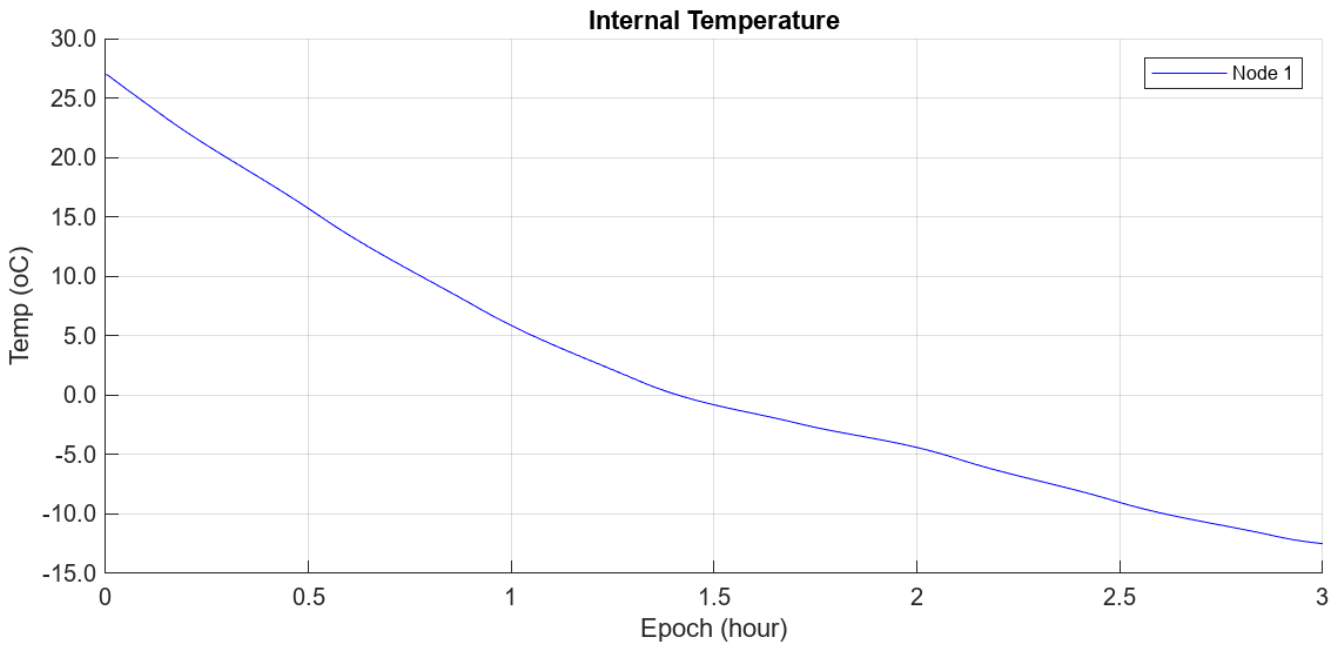
Figure 69: Internal Temperature for transient CMEx (and COM_CMEx) Mode and albedo coefficient of 0,7.

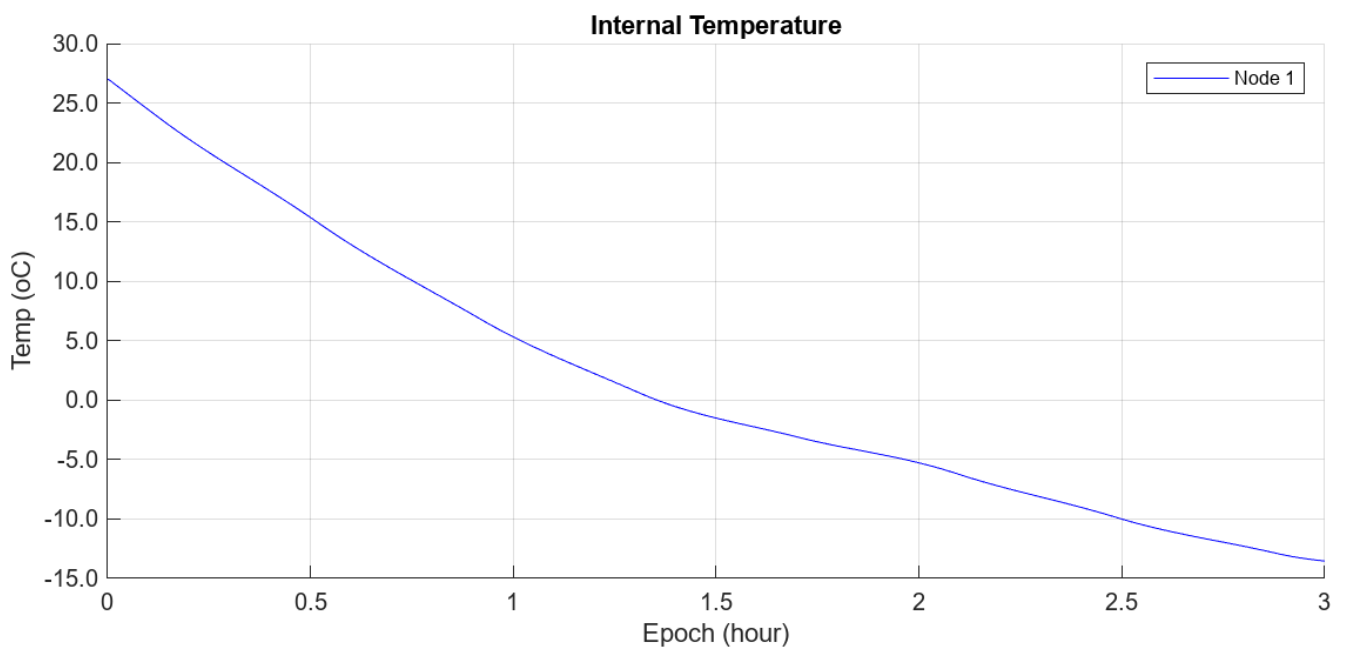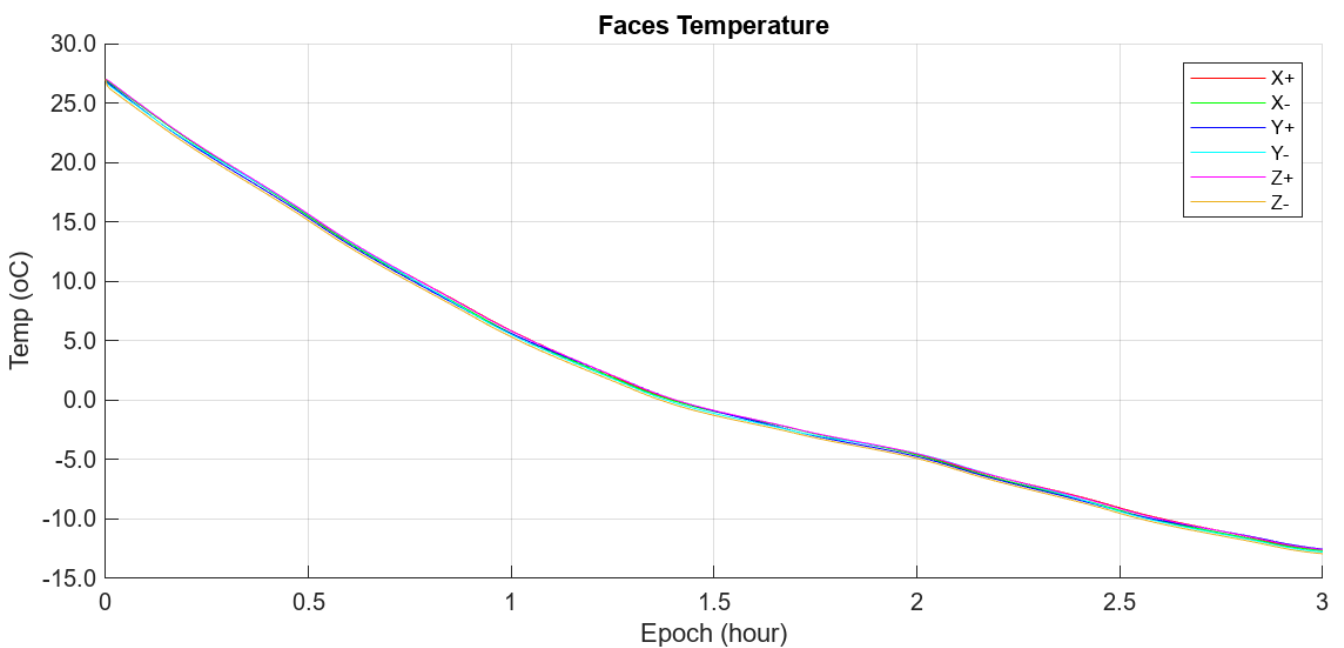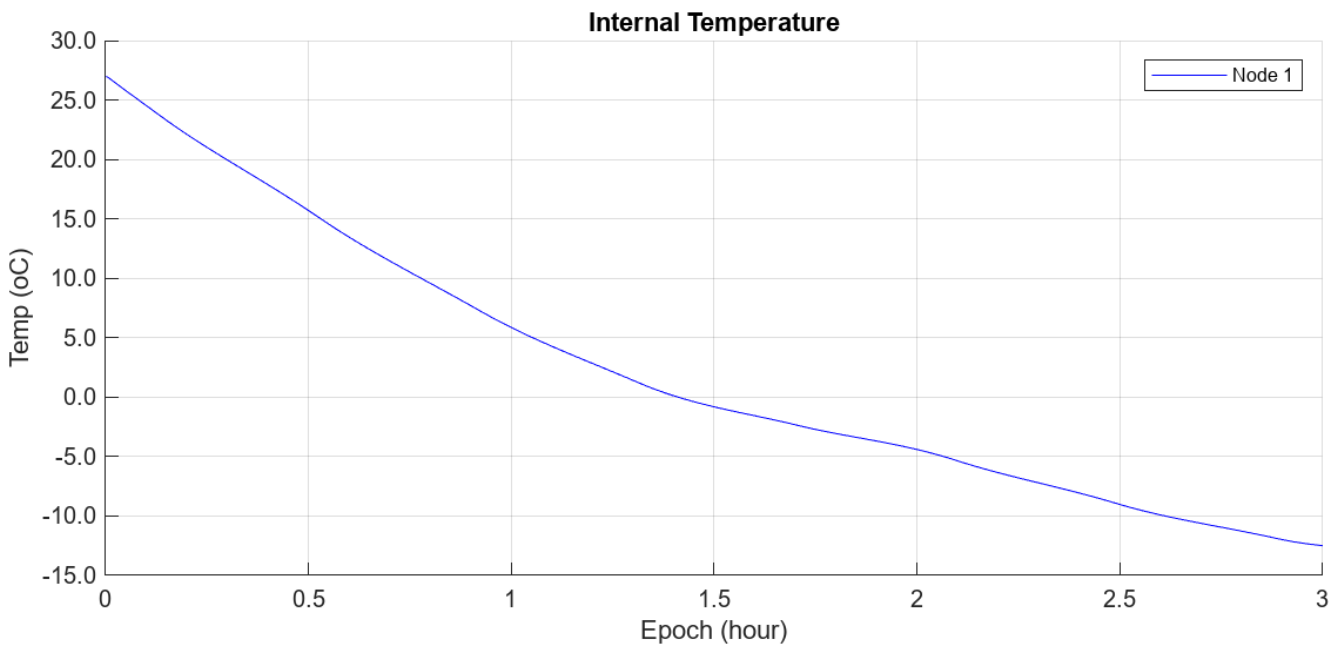Figure 70: Internal Temperature for transient CMEx (and COM_CMEx) Mode and albedo coefficient of 0,8.

From Figure 65, Figure 66, Figure 67, Figure 68, Figure 69 and Figure 70 the same exact conclusions can be drawn as for the COM and MAX_CHARGE analysis, but in this case, the values are a little bit higher due to the higher power consumption in CMEx and COM_CMEx modes, as shown in Table 2.

4. Conclusions and Further Steps

With all the results obtained, and taking into account only the transient study because it has higher precision than the steady study since many simplifications are made in the steady case, it can be determined the most critical cases for the TRACE CubeSat.

The higher temperature that TRACE satellite suffers occurs when the CubeSat is in any of the four operating modes as it can be seen in section 3.2, and this temperature is almost 30 °C. By the lower limit, the lowest temperature that TRACE satellite suffers occurs when the satellite is in COM or MAX_CHARGE operating modes, due to its lower power consumption and thus lower heat radiation. The lowest temperature that the satellite suffers is approximately -15 °C.

As it has been stated previously, TRACE CubeSat is formed of many components (Figure 7), but there are components that are more critical than others. For a CubeSat, the most critical subsystem is the power subsystem. [41]The two main components of the power subsystem are the batteries and the solar panels. The batteries supply power to all the other components of the CubeSat so they can continue operating when some failures or eclipses occur during the satellite's orbit, and the solar panels are designed to always face the Sun so they can recharge the batteries when needed. Another very critical component of TRACE CubeSat is the transceiver. [42]In the case of TRACE CubeSat, the batteries used are iEPS type B from ISISPACE [43], the solar panels used for TRACE are COTS assemblies from Azur Space formed of GaAs cells with an efficiency of 29,3% [33] [44], and finally TRACE utilizes a VHF uplink/UHF downlink Full Duplex Transceiver from ISISPACE. [45] The temperature ranges of the three critical components of TRACE CubeSat can be found in Table 4.

	TEMPERATURE [℃]	
	Minimum	Maximum
Solar Panels	-150	+150
Batteries	-40	+80
ISIS Transceiver	-20	+60

Table 4: Temperature range of TRACE critical components: Solar Panels and Batteries.

Looking at the temperature ranges of all the three critical components, it can be determined that the most critical component is the Transceiver, because its temperature range is lower than that of the other two components, its minimum temperature is the highest of the three components and the maximum temperature is the lowest of the three. Taking into account the results obtained in section 3.2, it can be said that TRACE CubeSat does not need any type of thermal control system installed. However, the minimum temperature achieved in the results is almost -15 ℃, which is near the minimum temperature limit for the Transceiver, so one possible solution to thermally isolate TRACE satellite and to effectively manage the temperature of the satellite is to use MLI since it is not a very expensive option. Another suitable option is the use of surface paintings, but in this case the paintings are more critical than the MLI since they need to possess sufficiently high thermal properties (emissivity and absorptivity) for the paint to last the entire TRACE mission without losing its thermal properties. [21]

In addition to the obtained results, a more extensive analysis is to be performed using specific and more precise software like ANSYS. With this type od software, more precise results are obtained but these analyses have been impossible to carry out due to licensing problems with the software, as stated in the introduction (1.1) of this master's thesis.

After all the thermal analysis performed in this report, some tests need to be made to validate the construction of TRACE CubeSat. In the thermal field, the tests to be carried out are the following ones: Thermal Vacuum Test, Thermal Cycle Test and finally Thermal Balance Test.

The Thermal Vacuum Test, also called System Functional Test has the objective to demonstrate the system's ability to fulfil all functional requirements at extreme temperature. All units are tested individually before the satellite TV test, but it is the first time that satellite and its units operate together. [29] [46]

The Thermal Cycle Test is part of the Thermal Vacuum Test, and thus has the same main objective, with one added objective that is to verify the test item design with reference to workmanship errors and mechanical stresses. [29] [46]

Finally, the Thermal Balance Test has the objective to provide a set of temperature data to correlate the thermal mathematical model and to verify the thermal control subsystem (TCS) design. [29] [46]

Once the tests are completed and verified, TRACE satellite, from the point of view of the Thermal Control System, is capable of performing and finishing successfully the mission for which it is designed.

Bibliography

[1] "Valispace," [Online]. Available: https://tudsat.valispace.com/project/33/dashboard/default.

[2] "CubeSat," [Online]. Available: https://www.cubesat.org/cubesatinfo.

[3] A. Johnstone, "CubeSat Design Specification (1U - 12U) REV 14.1," The CubeSat Program, Cal Poly SLO, 2022.

[4] E. Kulu, «Nanosatellite & CubeSat Database,» 28 August 2021. [En línea]. Available: https://www.nanosats.eu/.

[5] NASA, "Integration, Launch and Deployment," NASA.

[6] D. Hill, «About CubeSat Launch Initiative,» NASA, 31 March 2023. [En línea]. Available: https://www.nasa.gov/content/about-cubesat-launch-initiative.

[7] D. Hill, "The CubeSat Launch Initiative Celebrates its 100th CubeSat Mission Deployment," NASA, 19 February 2020. [Online]. Available: https://www.nasa.gov/feature/the-cubesat-launch-initiative-celebrates-its-100th-cubesat-mission-deployment.

[8] E. S. Agency, "Fly Your Satellite! programme," ESA, [Online]. Available: https://www.esa.int/Education/CubeSats_-_Fly_Your_Satellite/Fly_Your_Satellite!_programme#description.

[9] E. S. Agency, "Educational Payload on the Vega Maiden Flight Call For CubeSat Proposals," 2008.

[10] M. R. Crook, "NPS CubeSat Launcher Design, Process and Requirements," Naval Postgraduate School, 2009.

[11] "P-POD CubeSat Ejector," The Planetary Society, [Online]. Available: https://www.planetary.org/space-images/p-pod_mk_i_5.

[12] P. S. Arroyo, "Mission and Thermal Analysis of the UPC CubeSat," 2009.

[13] SatCatalog, "CubeSat launch Costs," 10 December 2022. [Online]. Available: https://www.satcatalog.com/insights/cubesat-launch-costs/#:~:text=The%20cost%20for%20CubeSat%20deployment,for%20deployment%20and%20mission%20operations..

[14] K. CS and B. Kanungo, "CubeSats Cost-Effective Delivery," SP's-Aviation, May 2017. [Online]. Available: https://www.sps-aviation.com/story/?id=2060.

[15] J. Dean, «NASA seeks launchers for smallest satellites,» 16 May 2015. [En línea]. Available: https://eu.floridatoday.com/story/tech/science/space/2015/05/16/nasa-seeks-launchers-smallest-satellites/27392049/.

[16] L. David, "CubeSats: Tiny Spacecraft, Huge Payoffs," [Online]. Available: https://www.space.com/308-cubesats-tiny-spacecraft-huge-payoffs.html.

[17] S. Writers, «Space Daily: History of the CubeSat,» 23 August 2016. [En línea]. Available: https://www.spacedaily.com/reports/History_of_the_CubeSat_999.html.

[18] Michael, "List of CubeSat Satellite Missions," 7 August 2009. [Online]. Available: https://mtech.dk/thomsen/space/cubesat.php.

[19] «CubeSats,» 31 March 2022. [En línea]. Available: https://www.esa.int/Enabling_Support/Preparing_for_the_Future/Discovery_and_Preparation/CubeSats.

[20] «Active Thermal Control System,» 2018. [En línea]. Available: https://www.aero.iitb.ac.in/satelliteWiki/index.php/Active_Thermal_Control_System.

[21] "Passive Thermal Control System," 2018. [Online]. Available: https://www.aero.iitb.ac.in/satelliteWiki/index.php/Passive_Thermal_Control_System#cite_note-7.

[22] G. Porter, "ESA," 10 August 2016. [Online]. Available: https://www.esa.int/ESA_Multimedia/Images/2016/08/Multi-layer_insulation_blankets.

[23] J. L. Kessler, C. Torrez and D. Arias, "Lightweight Flexible Thermal Energy Management Panels for CubeSats, Phase I," 2016. [Online]. Available: https://techport.nasa.gov/view/89663.

[24] "Paraffin wax," Wikipedia, [Online]. Available: https://en.wikipedia.org/wiki/Paraffin_wax.

[25] "Paraffin wax," CPCL, 24 August 2023. [Online]. Available: https://cpcl.co.in/paraffin-wax/.

[26] Wikipedia, "Thermal COnduction," [Online]. Available: https://en.wikipedia.org/wiki/Thermal_conduction.

[27] J. E. Lai, "Thermal Analysis for a High Precision Pointing Helios CUbeSat," 2015.

[28] Wikipedia, "Thermal Radiation," [Online]. Available: https://en.wikipedia.org/wiki/Thermal_radiation.

[29] P. Hager, "Thermal Design & Verification," ESA, 2022.

[30] "Thermal design handbook - Part 1: View factors," ESA Requirements and Stansards Division, 2011.

[31] B. Mattos, "Cubesat Thermal Power Toolbox," 2023. [Online]. Available: https://github.com/mattost14/CubeSat-Thermal-Power-App/releases/tag/v1.2.5.

[32] "Lumped-Element Model," Wikipedia, [Online]. Available: https://en.wikipedia.org/wiki/Lumped-element_model.

[33] A. S. S. P. GmbH, "30% triple Junction GaAs Solar Cell Assembly," AZUR SPACE Solar Power GmbH, 2016.

[34] "Metals, Metalic Elements and Alloys - Thermal Conductivities," The Engineering ToolBox, [Online]. Available: https://www.engineeringtoolbox.com/thermal-conductivity-metals-d_858.html.

[35] "Gallium Arsedine (GaAs) Specifications," Lake Shore Cryotronics, [Online]. Available: https://www.lakeshore.com/docs/default-source/default-document-library/gallium-arsenide-gaas-transmission-curve-datasheet.pdf?sfvrsn=a610d3d9_2.

[36] G. Lebbink, "STS Interface Specification v2.1: ISIS CubeSat Structural Subsystem," ISIS, 2012.

[37] NASA, "Structure, Mechanisms, and Materials," NASA.

[38] M. Khan, "The Ultimate Guide to PCB Materials: Choosing the Best Fit for Your Electronics Project," Wevolver, 26 April 2023. [Online]. Available: https://www.wevolver.com/article/the-ultimate-guide-to-pcb-materials-choosing-the-best-fit-for-your-electronics-project.

[39] "FR4 Thermal Conductivity and Thermal Resistance in PCB," Hillaman Curtis, [Online]. Available: https://hillmancurtis.com/fr4-thermal-conductivity/.

[40] Y. Zeng, D. Chalise, S. D. Lubner, S. Kaur and R. S. Prasher, "A review of thermal physics and management inside lithium-ion batteries for high energy density and fast charging".

[41] C. Dalibot and S. Tustain, "The Preliminary Thermal Design for the SPEQTRE CubeSat," 2020.

[42] A. G. C. Guerra, D. Nodar-López and R. Tubó-Pardavila, "Thermal Analysis of the Electronics of a CubeSat Mission," 2018.

[43] ISISPACE, "ICEPS2 Datasheet: Compact Electrical Power System suitable for up to 3U XL CubeSat missions.," ISISPACE Group, 2022.

[44] «Azur Space Customer Information,» [En línea]. Available: https://www.azurspace.com/index.php/en/products/products-space/customer-information.

[45] ISISPACE, «ISISPACE,» [En línea]. Available: https://www.isispace.nl/product/isis-uhf-downlink-vhf-uplink-full-duplex-transceiver/.

[46] E. Secretariat, "Space Engineering: Testing," 31 May 2022.

[47] "National Physical Laboratory," [Online]. Available: https://www.npl.co.uk/resources/q-a/why-is-emissivity-important.

[48] "Merriam-Webster," [Online]. Available: https://www.merriam-webster.com/dictionary/absorptivity.

[49] E. Gregersen, "Specific Heat," Britannica, [Online]. Available: https://www.britannica.com/science/specific-heat.

Appendix A: MATLAB Code

```matlab
%% CODE FOR THE CALCULATION OF THE STATIONARY CASE FOR TRACE CUBESAT:

% Orbit: Direct Sunlight
% Solar Heat Flux: 1412.9
% Albedo Coefficient: 0.6
% Satelleite as a Black Body
clear all
clc

%% CUBESAT DATA:

height_SC = 183.8604; % [mm]
width = 95; % [mm]
depth = 99.1873; % [mm]
Atot = 2*(width*1*10^-3*depth*1*10^-3)+2*(width*1*10^-3*height_SC*1*10^-3)+2*(depth*1*10^-3*height_SC*1*10^-3);

%% DATA:
Rt = 6378;
h = 430:10:530;
sigma = 5.67E-8; % [W/m^2K^4]
Tinf = 3; % [K]

%% HEAT FLUXES:

Solar = 1366.1; % Solar heat Flux [W/m2]
A_Coeff = 0.6; % Albedo Coefficient
IR = sigma*T^4; % Earth Infrarred Heat

%% INTERNAL POWER:

Qi_COM = 2.1638; % [W]
Qi_CMEx = 2.4038; % [W]
Qi_COM_CMEx = 2.4038; % [W]
Qi_MAX_CHARGE = 2.1638; % [W]

%% CASES:

syms Ts
% 1 -> i = 97,33 degrees
% 2 -> i = 90 degrees
% 3 -> i = 0 degrees

caso = 3; % Can be 1, 2 or 3
temperature = 2; % Can be 1 (260 K) or 2 (240 K)

if caso == 1 && temperature == 1
    i = 97.33; % [Degrees]
    lambda1 = i-90; % [Degrees]
    lambda2 = 180-i; % [Degrees]
    angle = 180-90-(i-90); % [Degrees]
```

```matlab
        h1 = depth*sind(i-90); % [mm]
        h2 = height_SC*cosd(i-90); % [mm]
        A1 = h1*width; % [mm^2]
        A2 = h2*width; % [mm^2]
        Asun = A1+A2; % [mm^2]
        Qsun = Solar*Asun*1*10^-6; % [W]
        for x = 1:length(h)
            F12_1(x) = cosd(lambda1)/(1+h(x)/Rt).^2;
            Qearth1(x) = sigma*260^4*(depth*width)*1*10^-6*F12_1(x); % [W]
            Qalbedo1(x) = Solar*A_Coeff*(depth*width)*1*10^-6*F12_1(x); % [W]
        end

        for y = 1:length(h)
            F12_2(y) = cosd(lambda2)/(1+h(y)/Rt).^2;
            Qearth2(y) = sigma*260^4*(height_SC*width)*1*10^-6*F12_1(y); % [W]
            Qalbedo2(y) = Solar*A_Coeff*(height_SC*width)*1*10^-6*F12_1(y); % [W]
        end
        Qearth = Qearth1+Qearth2; % [W]
        Qalbedo = Qalbedo1+Qalbedo2; % [W]

elseif caso == 1 && temperature == 2
        i = 97.33; % [Degrees]
        lambda1 = i-90; % [Degrees]
        lambda2 = 180-i; % [Degrees]
        angle = 180-90-(i-90); % [Degrees]
        h1 = depth*sind(i-90); % [mm]
        h2 = height_SC*cosd(i-90); % [mm]
        A1 = h1*width; % [mm^2]
        A2 = h2*width; % [mm^2]
        Asun = A1+A2; % [mm^2]
        Qsun = Solar*Asun*1*10^-6; % [W]
        for x = 1:length(h)
            F12_1(x) = cosd(lambda1)/(1+h(x)/Rt).^2;
            Qearth1(x) = sigma*240^4*(depth*width)*1*10^-6*F12_1(x); % [W]
            Qalbedo1(x) = Solar*A_Coeff*(depth*width)*1*10^-6*F12_1(x); % [W]
        end

        for y = 1:length(h)
            F12_2(y) = cosd(lambda2)/(1+h(y)/Rt).^2;
            Qearth2(y) = sigma*240^4*(height_SC*width)*1*10^-6*F12_1(y); % [W]
            Qalbedo2(y) = Solar*A_Coeff*(height_SC*width)*1*10^-6*F12_1(y); % [W]
        end
        Qearth = Qearth1+Qearth2; % [W]
        Qalbedo = Qalbedo1+Qalbedo2; % [W]

elseif caso == 2 && temperature == 1
        i = 90; % [Degrees]
        lambda = 0; % [Degrees]
        angle = 180-i-(i-90); % [Degrees]
        h1 = depth*sind(i-90); % [mm]
        h2 = height_SC*cosd(i-90); % [mm]
        A1 = h1*width; % [mm^2]
        A2 = h2*width; % [mm^2]
        Asun = A1+A2; % [mm^2]
        Aearth = width*depth; % [mm^2]
        Aalbedo = Aearth; % [mm^2]
        for x = 1:length(h)
```

```matlab
        F12(x) = cosd(lambda1)/(1+h(x)/Rt).^2;
    end
    Qsun = Solar*Asun*1*10^-6; % [W]
    Qearth = sigma*260^4*Aearth*1*10^-6*F12; % [W]
    Qalbedo = Solar*A_Coeff*Aalbedo*1*10^-6*F12; % [W]

elseif caso == 2 && temperature == 2
    i = 90; % [Degrees]
    lambda = 0; % [Degrees]
    angle = 180-i-(i-90); % [Degrees]
    h1 = depth*sind(i-90); % [mm]
    h2 = height_SC*cosd(i-90); % [mm]
    A1 = h1*width; % [mm^2]
    A2 = h2*width; % [mm^2]
    Asun = A1+A2; % [mm^2]
    Aearth = width*depth; % [mm^2]
    Aalbedo = Aearth; % [mm^2]
    for x = 1:length(h)
        F12(x) = cosd(lambda1)/(1+h(x)/Rt).^2;
    end
    Qsun = Solar*Asun*1*10^-6; % [W]
    Qearth = sigma*240^4*Aearth*1*10^-6*F12; % [W]
    Qalbedo = Solar*A_Coeff*Aalbedo*1*10^-6*F12; % [W]

elseif caso == 3 && temperature == 1
    i = 0; % [Degrees]
    lambda = 90; % [Degrees]
    angle = 90-i-(i-90); % [Degrees]
    h1 = depth*sind(90-i); % [mm]
    h2 = height_SC*cosd(90-i); % [mm]
    A1 = h1*width; % [mm^2]
    A2 = h2*width; % [mm^2]
    Asun = A1+A2; % [mm^2]
    Aearth = height_SC*width; % [mm^2]
    Aalbedo = Aearth; % [mm^2]
    for x = 1:length(h)
        F12(x) = cosd(lambda2)/(1+h(x)/Rt).^2;
    end
    Qsun = Solar*Asun*1*10^-6; % [W]
    Qearth = sigma*260^4*Aearth*1*10^-6*F12; % [W]
    Qalbedo = Solar*A_Coeff*Aalbedo*1*10^-6*F12; % [W]

elseif caso == 3 && temperature == 2
    i = 0; % [Degrees]
    lambda = 90; % [Degrees]
    angle = 90-i-(i-90); % [Degrees]
    h1 = depth*sind(90-i); % [mm]
    h2 = height_SC*cosd(90-i); % [mm]
    A1 = h1*width; % [mm^2]
    A2 = h2*width; % [mm^2]
    Asun = A1+A2; % [mm^2]
    Aearth = height_SC*width; % [mm^2]
    Aalbedo = Aearth; % [mm^2]
    for x = 1:length(h)
        F12(x) = cosd(lambda2)/(1+h(x)/Rt).^2;
    end
    Qsun = Solar*Asun*1*10^-6; % [W]
```

```matlab
        Qearth = sigma*260^4*Aearth*1*10^-6*F12; % [W]
        Qalbedo = Solar*A_Coeff*Aalbedo*1*10^-6*F12; % [W]

end

Qext = Qsun + Qearth + Qalbedo; % [W]
Qout = Atot*sigma*(Ts^4-Tinf^4); % [W]

%% MODE CALCULATIONS:
clear T
mode = 1; % 1 -> COM; 2 -> CMEx; 3 -> COM_CMEx; 4 -> MAX_CHARGE

if mode == 1
    Qin = Qext + Qi_COM; % [W]
    eq = Qin == Qout;
    for x = 1:length(eq)
        T(:,x) = double(solve(eq(x),Ts));
    end
    T = T(2,:); % [K]
    figure
    plot(T,'b--')
    title('COM Mode')
    ylabel('Temperature [K]')
    xlabel('Altitude [Km]')

xticklabels({'430','440','450','460','470','480','490','500','510','520','530'})
elseif mode == 2
    Qin = Qext + Qi_CMEx; % [W]
    eq = Qin == Qout;
    for x = 1:length(eq)
        T(:,x) = double(solve(eq(x),Ts));
    end
    T = T(2,:); % [K]
    figure
    plot(T,'b--')
    title('CMEx Mode')
    ylabel('Temperature [K]')
    xlabel('Altitude [Km]')

xticklabels({'430','440','450','460','470','480','490','500','510','520','530'})
elseif mode == 3
    Qin = Qext + Qi_COM_CMEx; % [W]
    eq = Qin == Qout;
    for x = 1:length(eq)
        T(:,x) = double(solve(eq(x),Ts));
    end
    T = T(2,:); % [K]
    figure
    plot(T,'b--')
    title('COM-CMEx Mode')
    ylabel('Temperature [K]')
    xlabel('Altitude [Km]')

xticklabels({'430','440','450','460','470','480','490','500','510','520','530'})
elseif mode == 4
    Qin = Qext + Qi_MAX_CHARGE; % [W]
    eq = Qin == Qout;
```

```matlab
    for x = 1:length(eq)
        T(:,x) = double(solve(eq(x),Ts));
    end
    T = T(2,:); % [K]
    figure
    plot(T,'b--')
    title('MAX-CHARGE Mode')
    ylabel('Temperature [K]')
    xlabel('Altitude [Km]')

xticklabels({'430','440','450','460','470','480','490','500','510','520','530'})
end
```

Appendix B: Definitions

Emissivity: emissivity is the dimensionless ratio of energy emitted by a material's surface to that emitted by a black body, a perfect emitter, at the same temperature, wavelength, and viewing conditions. It ranges from 0 (for a perfect reflector) to 1 (for a perfect emitter), defining a material's radiative properties. [47]

Absorptivity: is the property of a body that determines the fraction of incident radiation absorbed by the body. [48]

Specific Heat: the quantity of heat required to raise the temperature of one gram of a substance by one Celsius degree. [49]